SLL 80-392/M

(8)

Project Report

PA-385

M. J. Lewis

Recognition of a Target on an ARWBC RTI

12 November 1976

Prepared for the Department of the Air Force
under Electronic Systems Division Contract F19628-76-C-0002 by

Lincoln Laboratory

MASSACHUSETTS INSTITUTE OF TECHNOLOGY

LEXINGTON, MASSACHUSETTS

19980513 104

Approved for public release; distribution unlimited.

The work reported in this document was performed at Lincoln Laboratory, a center for research operated by Massachusetts Institute of Technology, with the support of the Department of the Air Force under Contract F19628-76-C-0002.

Accession Number: 3780

Publication Date: Nov 12, 1976

Title: Recognition Of A Target On An ARWBC RTI

Personal Author: Lewis, M.J.

Corporate Author Or Publisher: Lincoln Laboratory, M.I.T., P.O. Box 73, Lexington, MA 02173 Report Number: PA-385 Report Number Assigned by Contract Monitor: SLL 80-392/M

Comments on Document: Archive, RRI, DEW

Descriptors, Keywords: Directed Energy Weapon DEW Target ARWBC RTI

Pages: 00043

Cataloged Date: Oct 08, 1992

Contract Number: F19628-76-C-0002

Document Type: HC

Number of Copies In Library: 000001

Record ID: 24928

Source of Document: DEW

MASSACHUSETTS INSTITUTE OF TECHNOLOGY

LINCOLN LABORATORY

RECOGNITION OF A TARGET ON AN ARWBC RTI

M. J. LEWIS

Group 92

PROJECT REPORT PA-385

12 NOVEMBER 1976

LEXINGTON MASSACHUSETTS

ABSTRACT

The task faced by the All-Range WideBand Channel (ARWBC) operator at ALCOR while trying to detect the presence and location of a target of interest on the RTI display was examined with the aid of digital RTIs produced by a computer simulation. Controlled levels of three degrading factors --- background clutter, missed target returns, and an unsteady target track --- were produced in the simulation RTIs and a subjective judgment made as to which RTIs contained detectable target tracks. In this way, useful limits were established on tolerable levels of the three degrading factors considered.

TABLE OF CONTENTS

I. INTRODUCTION

The All-Range Wide-Band Channel (ARWBC) is a component of the ALCOR radar designed to provide range coverage greater than that available with the conventional ALCOR wide-band window (90 m), and to test designation techniques in real-time. One output of the ARWBC is a digital RTI displaying those range positions in each pulse interval where a target is detected. (A target detection is determined by a return satisfying a preselected set of thresholds on amplitude, length, etc.)

An important question in the operation of the ARWBC is the ability of an operator to view the digital RTI and detect the existence and location of a target. Several possible factors hamper this detection, the most important being:

The amount of background clutter.

The proportion of returns missing from the target trace.

The extent to which the target return, when present, wanders about on the face of the RTI.

The detection problem faced by the operator---basically a psychological one---is investigated in this report through the use of simulated RTIs which contain the degrading factors to controlled levels. Although the decision as to whether a particular RTI would thwart or permit detection is a subjective one, it is believed that the ground rules developed in this report establish useful limits on the levels of the degrading factors. The ground rules apply equally well to RTI displays other than that of the ARWBC.

II. DESCRIPTION OF PROBLEM

An RTI can allow an observer to follow the track of a target provided that the tracking gate is being accurately designated along the trajectory of the target. Figure 1 shows a computer simulation of such an RTI, where time in seconds runs along the vertical axis (increasing upwards) and range in meters relative to the tracking gate is displayed along the horizontal axis. After an initial range displacement at time 0,

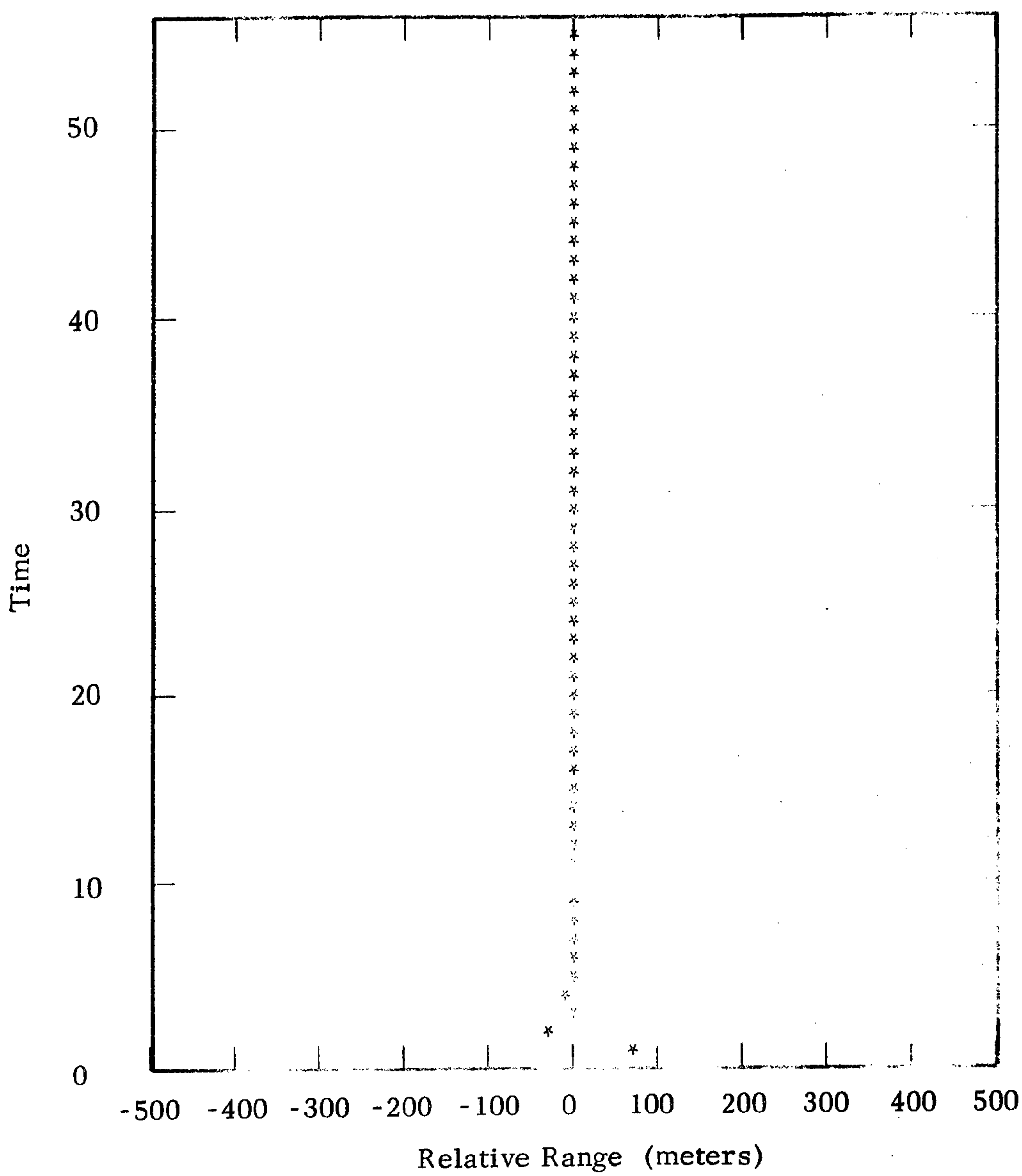

Fig. 1. RTI without degrading factors.

the tracking gate is accurately designated on the target trajectory and the line of asterisks continues up the center of the RTI. The straightness of the line is an indication of the precision of the designation source. Because there are no other targets in the environment, the rest of the screen is clear. Because all of the target returns passed the thresholds of the RTI system, the line is continuous.* Under such conditions, it is an easy matter for an observer to follow the target path.

But the situation is not always so simple. Several factors can complicate the task of detection for the observer. First, depending on the thresholds built into the ARWBC algorithms, some of the returns from the target of interest may not pass the algorithms, and gaps may appear in the line. These will be called "missed returns." More important, an environment filled with penetration aids or clutter may cause additional returns in each range sweep which can obscure the path of the target of interest. In a typical situation, the clutter might consist of several kilometers of chaff, and the target of interest might be an RV. In this report we will occasionally refer to the problem of detecting an RV imbedded in chaff, keeping in mind that the conclusions to be drawn apply to any general detection problem.

In addition to clutter and missed returns, a third factor working against the observer is track wander. Depending on the source of designation information being provided to the ARWBC, the target of interest may wander within the RTI range sweep. For example, the ARWBC may be designated by a beacon track. In this case, the target skin return will generally be at a constant range relative to the beacon, with very small range deviations due to beacon instabilities, and the operator will have little trouble following the target through moderate chaff, even with some missed target returns. But in a scenario more realistic from the defense point of view, ARWBC designation would not be provided by a beacon, but perhaps by a track of the centroid of the surrounding chaff cloud. In general, chaff trackers are characterized by substantial range residuals. That is, at any given time, the tracking gate of a chaff tracker may be offset by a

* Unfortunately, some of the asterisks may not have passed the threshold of our reproduction facilities.

substantial amount from the actual physical centroid of the cloud, which is moving smoothly through space. These offsets will be random in nature, hopefully with zero mean, and with some standard deviation which is a measure of the precision of the chaff track. Since the RV is presumably fixed relative to the cloud centroid,* the RTI tracking gate range offsets relative to the cloud centroid will be translated into range offsets relative to the RV, causing the RV returns to wander across the face of the RTI. Thus, the standard deviation of the tracker range residuals will impact on the task of the RTI observer. Figure 2 shows a digital RTI in which clutter fills approximately 20% of the screen, 10% of the returns from the RV imbedded in the clutter have been deleted, and a small amount of track wander has been introduced. An observer would require a great deal of imagination to pick out the path of the RV.

The purpose of this report is to investigate the impact of these three degrading factors---missed returns, clutter, and target track wander---on the detection problem faced by the RTI observer. By use of a computer program which produces simulated digital RTIs, RTI plots containing controlled amounts of the three factors were produced, and a decision was made as to whether or not the target track was detectable.

A track was considered detectable if the observer could correctly determine the position of the target roughly 50% of the time. It must be stressed that the detection decision was purely subjective. Another observer might find it harder or easier to see the target. A criterion other than 50% might be used. Despite the subjectivity involved, it is believed that this approach can establish useful allowable limits on the three degrading factors investigated.

III. COMPUTER MODEL OF TRACK WANDER, LEAKAGE, AND CLUTTER

A computer program was designed to produce simulated digital RTI plots containing controlled amounts of the three degrading factors. The wandering track that

* Or at worst having a smooth velocity relative to the centroid.

PA-385 (2)

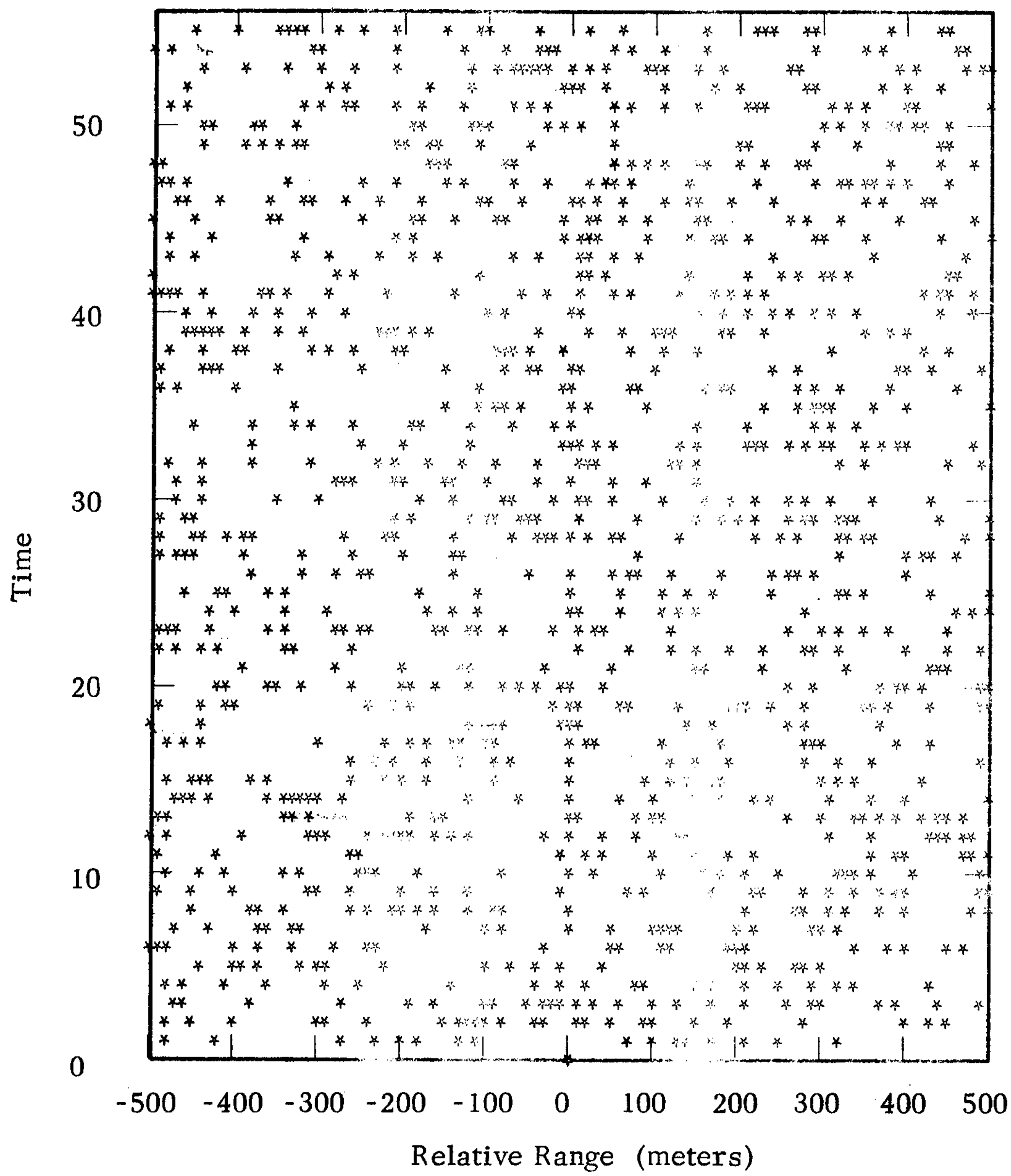

Fig. 2. RTI with unsteady track, missed returns and clutter.

would be produced by a designation source less steady than a beacon was modeled as a second-order autoregressive discrete time process with zero mean and Gaussian white noise. That is, at time k Δ, where Δ is the interpulse period and k = 0, 2, . . . , 55,* the range offset, X_k, from the center of the RTI is given by

$$X_k = \alpha_1 X_{k-1} + \alpha_2 X_{k-2} + N_k$$

where α_1 and α_2 are constants and N_k is a Gaussian random variable with zero mean and standard deviation σ_N. Each point in the series depends explicity on the two previous points. Points were plotted as integer values, but rational values of X_k were retained for calculation of X_{k+1} and X_{k+2}. In order for the process to be stationary, α_1 and α_2 must satisfy the following conditions:

$$\alpha_1 + \alpha_2 < 1$$

$$\alpha_1 - \alpha_2 > -1$$

$$-1 < \alpha_2 < 1$$

If the sequence X_k is stationary, its mean will remain zero and its standard deviation, which is a measure of the wander of the track about the mean, is given by

$$\sigma_x = \sqrt{\frac{1 - \alpha_2}{1 - \alpha_2 - \alpha_2^2 + \alpha_2^3 - \alpha_1^2 \alpha_2 - \alpha_1^2}} \; \sigma_N^{**}$$

In order to manufacture assorted values of σ_x to provide simulations of progressively unsteady tracks, one can manipulate α_1, α_2, or σ_N. The relevant quantity is σ_x. It is a measure of the wander of the RV track across the RTI, since roughly

* The upper limit of 55 is governed by the physical height of the RTI presentation on each page.

** See Appendix A for derivation.

95% of the RV returns should lie within 2 σ_x units of the origin. Because the dependence of σ_x on σ_N is more straightforward than that on α_1 or α_2, σ_x was varied by manipulating σ_N while holding α_1 and α_2 constant. Values of $(\alpha_1, \alpha_2) = (0.8, -0.2)$ were found to be convenient, reducing the constant of proportionality in the last equation to 1.37.

At this point, it is instructive to consider what values of σ_x might be of interest. Previous chaff tracking performance of the KREMS radars* was explored. The TRADEX L-chirp waveform typically produces range residuals on the order of 30 meters. ALTAIR, using its video Track Signal Processor, has produced range residuals on the order of 150 m. With its new Digital Track Signal Processor, the ALTAIR range residuals have been reduced to fractions of one meter, which would be undetectable on the range scale used. Thus, in order to provide a representative range of values of 2 σ_x, six values of σ_N from 0 to 50 meters were input to the computer program. Corresponding values of 2 σ_x are shown below. It was assumed that the chaff tracking performance of any defense radar would lie somewhere in this range.

σ_N(m)	2 σ_x(m)
0	0
5	14
10	27
20	55
30	82
50	137

In addition to the wandering target track determined by the autoregressive process described above, missed returns and clutter models were included in the computer simulation. Missed returns were inserted by the following mechanism: before

* See Appendix B for radar characteristics.

each point in the target track was plotted, a random number selected from a uniform distribution was compared with a preset threshold called T2. For example, if T2 were set to 0.3, 30% of the target returns were randomly deleted from the plot. Clutter was randomly scattered across the page via a similar comparison between a preset clutter threshold and another uniformly distribution random variable at each (range, time) coordinate on the page. For example, a clutter threshold of 0.2 resulted in 20% of the page being filled with asterisks.

IV. COMPUTER-GENERATED PLOTS

Figures C-1 to C-5 show plots generated by the simulation program with values of σ_N = 0, 5, 10, 20, 30, and 50, respectively. There is no clutter, and all returns were printed. Values of α_1, α_2, the clutter threshold, percentage of missed returns, σ_N and $2\sigma_x$ are shown at the bottom of the figures. Using these as baselines plots, progressively greater levels of clutter and missed returns were added by manipulation of the clutter level up to 10% and missed returns up to 50%, and judgments were made as to when the unsteady track became undetectable to the eye. A track was considered detectable if at least 50% of the target returns were distinguishable from clutter. These judgments were, of course, subjective.

Table I summarizes the outcome of the examination of each plot. For each combination of $2\sigma_x$, clutter level, and missed returns shown, there is an indication as to which RTIs contained detectable tracks (X) and which RTIs did not (O). A selection of RTIs for the reader's inspection are provided in Appendix C and indexed by figure number in Table I.

V. CONCLUSIONS

Figure 3 presents a summary of the results tabulated in Table I. For fixed values of $2\sigma_x$, the highest tolerable level of missed returns was plotted against clutter. For example, at 8% clutter, RTIs with $2\sigma_x$ = 14 meters contained detectable

TABLE I

RTI EXAMINATION RESULTS

σ_N	$2\sigma_x$	Clutter (%)	Missed Returns (%)	Result*	Figure
0	0	1	0	X	
			10	X	
			20	X	
			30	X	
			40	X	
			50	X	C-6
		2	0	X	
			10	X	
			20	X	
			30	X	
			40	X	
			50	X	C-7
		4	0	X	
			10	X	
			20	X	
			30	X	
			40	X	
			50	X	C-8
		6	0	X	
			10	X	
			20	X	
			30	X	
			40	X	C-9
			50	O	
		8	0	X	
			10	X	
			20	X	
			30	X	
			40	X	
			50	O	C-10

* X = Detectable Track; O = Undetectable Track.

σ_N	$2\sigma_x$	Clutter (%)	Missed Returns (%)	Result*	Figure
0	0	10	0	X	
			10	X	
			20	X	
			30	X	
			40	O	
			50	O	
5	14	1	0	X	
			10	X	
			20	X	
			30	X	
			40	X	
			50	X	C-11
		2	0	X	
			10	X	
			20	X	
			30	X	
			40	X	C-12
			50	O	
		4	0	X	
			10	X	
			20	X	
			30	X	
			40	O	C-13
			50	O	
		6	0	X	
			10	X	C-14
			20	X	
			30	O	
			40	O	
			50	O	
		8	0	X	
			10	X	
			20	O	C-15
			30	O	

* X = Detectable Track; O = Undetectable Track.

σ_N	$2\sigma_x$	Clutter (%)	Missed Returns (%)	Result*	Figure
5	14	10	0	X	
			10	X	
			20	O	
			30	O	
10	27	1	0	X	
			10	X	
			20	X	
			30	X	
			40	X	
			50	O	C-16
		2	0	X	
			10	X	
			20	X	
			30	X	
			40	O	C-17
			50	O	
		4	0	X	
			10	X	
			20	O	
			30	O	
			40	O	
		6	0	X	C-18
			10	O	
			20	O	
			30	O	
		8	0	X	C-19
			10	O	
			20	O	
		10	0	O	
			10	O	
20	55	1	0	X	
			10	X	
			20	X	C-20
			30	O	

* X = Detectable Track; O = Undetectable Track.

σ_N	$2\sigma_x$	Clutter (%)	Missed Returns (%)	Result*	Figure
20	55	2	0	X	
			10	O	C-21
			20	O	
		4	0	O	
			10	O	
		6	0	O	C-22
			10	O	
		8	0	O	
			10	O	
		10	0	O	
			10	O	
30	82	1	0	X	
			10	X	C-23
			20	O	
			30	O	
		2	0	O	C-24
			10	O	
		3	0	O	
		4	0	O	
			10	O	
50	137	1	0	O	C-25
			10	O	
		2	0	O	
			10	O	

* X = Detectable Track; O = Undetectable Track.

PA-385 (3)

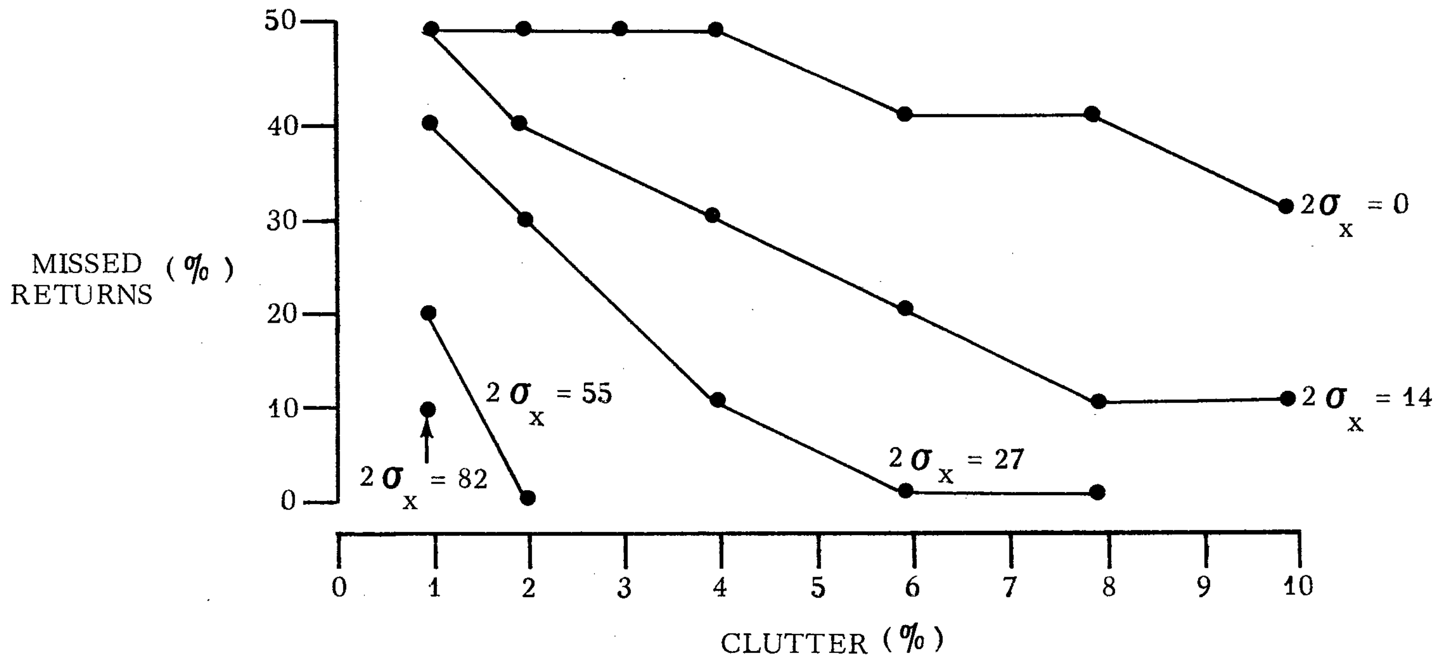

Fig. 3. Summary of detectable tracks: points plotted represent highest level of missed returns tolerated as a function of clutter for fixed values of $2\sigma_x$.

tracks with fraction missed of up to 10%. Missed returns over 10% rendered the track undetectable. No curve appears for $2\sigma_x = 137$, as none of the tracks from that group were detectable. Not surprisely, the highest tolerable level of missed returns falls off with increasing clutter and increasing track wander. The rate of falloff of maximum missed returns with clutter varies from gradual in the case of a steady track ($2\sigma_x = 0$) to rapid in the case of more unsteady tracks ($2\sigma_x \geq 55$).

In summary, an observer trying to detect returns on an RTI from a target of interest imbedded in clutter faces several obstacles. Range displacements relative to the RTI origin may be introduced by the designation information provided by the radar tracker. Clutter and missing returns obscure the path of the target. With a designation source which introduces range displacements of standard deviation greater than a few tens of meters, the range of tolerable clutter and missing returns is severely limited. Limits of tolerable track wander, clutter, and missing returns derived from subjective criteria are displayed in Figure 3.

ACKNOWLEDGMENT

I wish to express my thanks to Linda Simon, who wrote the computer program used to generate the simulation RTIs contained in this report.

APPENDIX A

Derivation of σ_x

N_k is a sequence of Gaussian random numbers with mean zero and standard deviation σ_N

X_k is a second-order auto-regressive discrete time sequence with zero mean and Gaussian white noise. That is,

$$X_k = \alpha_1 X_{k-1} + \alpha_2 X_{k-2} + N_k$$

We wish to find an expression for σ_x in terms of α_1, α_2, and σ_N.

$$\sigma_x^2 = E[x_k^2] = E[(\alpha_1 x_{k-1} + \alpha_2 x_{k-2} + N_k)^2]$$

$$= E[\alpha_1^2 x_{k-1}^2 + \alpha_2^2 x_{k-2}^2 + 2\alpha_1 \alpha_2 x_{k-1} x_{k-2} + N_k^2 +$$

$$2(\alpha_1 x_{k-1} + \alpha_2 x_{k-2}) N_k]$$

$$= \alpha_1^2 E[x_{k-1}^2] + \alpha_2^2 E[x_{k-2}^2] + 2\alpha_1 \alpha_1 E[x_{k-1} x_{k-2}] + \sigma_N^2$$

$$E[x_{k-1}^2] = E[x_{k-2}^2] = E[x_k^2] = \sigma_x^2$$

$$\text{Cov}[x_k, x_{k-1}] = E[x_k \; x_{k-1}] = E[\alpha_1 x_{k-1}^2 + \alpha_2 x_{k-1} x_{k-2} + x_{k-1} N_k]$$

$$= \alpha_1 \sigma_x^2 + \alpha_2 \text{Cov}[x_k, x_{k-1}]$$

Solving for $\text{Cov}[x_k, x_{k-1}]$,

$$\text{Cov}[x_k, x_{k-1}] = \frac{\alpha_1}{1-\alpha_2} \sigma_x^2$$

Thus,

$$\sigma_x^2 = \alpha_1^2 \sigma_x^2 + \alpha_2^2 \sigma_x^2 + 2\alpha_1 \alpha_2 \frac{\alpha_1}{1-\alpha_2} \sigma_x^2 + \sigma_N^2$$

Solving for σ_x^2,

$$\sigma_x^2 = \frac{1 - \alpha_2}{1 - \alpha_2 - \alpha_2^2 + \alpha_2^3 - \alpha_1^2 \alpha_2 - \alpha_1^2} \quad \sigma_N^2$$

$$\boxed{\sigma_x = \sqrt{\frac{1 - \alpha_2}{1 - \alpha_2 - \alpha_2^2 + \alpha_2^3 - \alpha_1^2 \alpha_2 - \alpha_1^2}} \quad \sigma_N}$$

APPENDIX B

RADAR CHARACTERISTICS

	ALTAIR			ALCOR		TRADEX			
	Waveform	VHF	UHF	Waveform	C-band	Waveform	L-band	Waveform	S-band
Beamwidth (6 dB-two way)		3°	1°		0.41°		0.65°		0.25°
Frequency (MHz)		155.5	415	NB	5664		1320		2950.8
				WB	5659				
Peak Power (MW)		10	20		2.5		1.75		2.6
PRF		40-6900	40-3000		11-200		94-1500		94-1500
Transmitted Pulsewidth (μs)	Long Chirp	30	15		10	Chirp	50	Chirp/Pulse Pair	9
	Short Chirp	6	3			LIDAR	2	WB Chirp	3
	CW	0.25	0.1			Burst*	2	Burst*	3
	CWL	30	16					DUBurst 20	2
	UA		25						
	UB		25						
Chirp Ramps (MHz)		7	17.5	NB	5.99	Chirp	1	Chirp/Pulse Pair	17.6
				WB**	512	LIDAR	20	WB Chirp	60
						Burst	20	Burst+	60
								DUBurst 20	20
Range Resolution (m) (6 dB-two way)	Long Chirp	37.5	15	NB	52.50	Chirp	240	Chirp	15
	Short Chirp	37.5	15	WB**	0.54	LIDAR	15	WB Chirp	5
	CW	37.5	15			Burst	15	Burst	5
	CWL	4500	2400					FJB	1
	UA		1200						
	UB		375						
Receiver Channels		LC, RC	LC, RC		LC, RC, Ref.	Chirp/	LC, RC	Chirp/Pulse Pair	LC, RC
		Az and El	Az and El		Az and El	LIDAR	Az and El	WB Chirp	LC, RC
		Error	Error		Error		Error	Burst	LC, RC
					Beacon	Burst	LC, RC	FJB	LC, RC
								DUBurst 20	LC
Range Doppler Coupling** (m) (V_d = 7.5 km/s)	Long Chirp	5	2.7	NB	72.5	Chirp	496.8	Chirp/Pulse Pair	11.3
	Short Chirp	1	0.5	WB	0.825	LIDAR	-1.0	WB Chirp	1.1
						Burst	-1.0	Burst	1.1
								DUBurst 20	2.2
Tracking Coordinates		R, Az, El	R, Az, El	NB	R, Az, El	Chirp	R, Az, El	Chirp/Pulse Pair	R
				WB	R, Az, El	LIDAR	R, Az, El		
				Beacon	R, Az, El				

*TRADEX Burst Waveforms are (at L-band): Burst, 2 to 32 pulses spaced at 14 μs (A Burst) or 28 μs (C Burst); at S-band: Burst, 2 to 32 pulses spaced 4 to 32 μs; FJB, 2 to 32 pulses spaced 4 to 32 μs with frequency steps (MHz) of 0, 9.6, 19.2, 28.8, 38.4, 48.0, and 57.6; DUBurst, 2 to 32 pulses spaced 4 to 25 μs, 20 or 60 MHz.

**AWB, WBQ, and AWBQ ALCOR waveforms have characteristics identical to WB.

+DUBurst 60 and FJB TRADEX waveforms have characteristics identical to S Burst.

APPENDIX C

Simulated RTIs

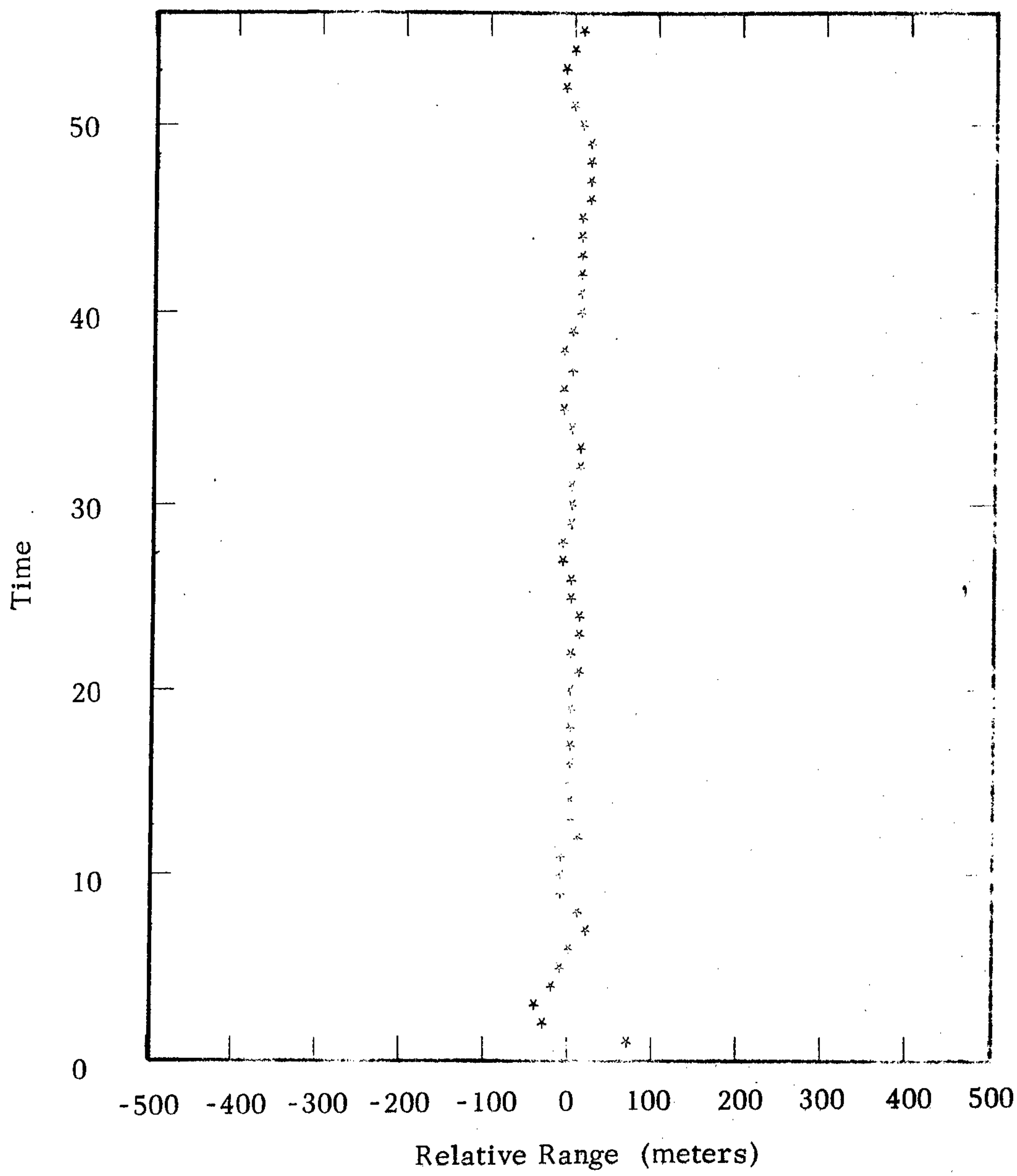

Clutter = 0% $\quad \alpha_1 = 0.80 \quad \sigma_N = 10$

Missed Returns = 0% $\quad \alpha_2 = -0.20 \quad 2\sigma_X = 27$

Fig. C-1. Unsteady target track.

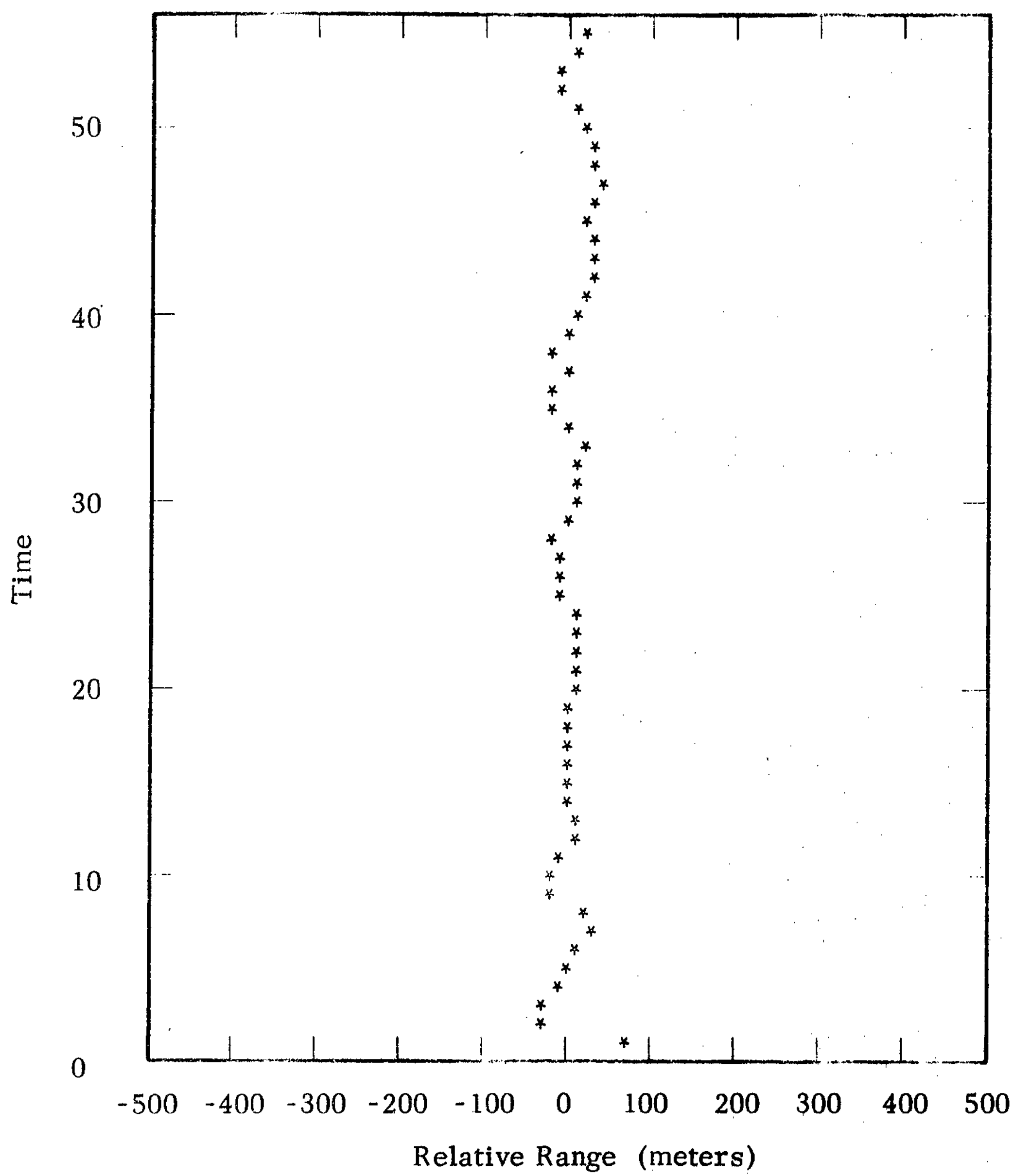

Clutter = 0% α_1 = 0.80 σ_N = 5

Missed Returns = 0% α_2 = -0.20 $2\sigma_X$ = 13

Fig. C-2. Unsteady target track.

PA-385 (C-3)

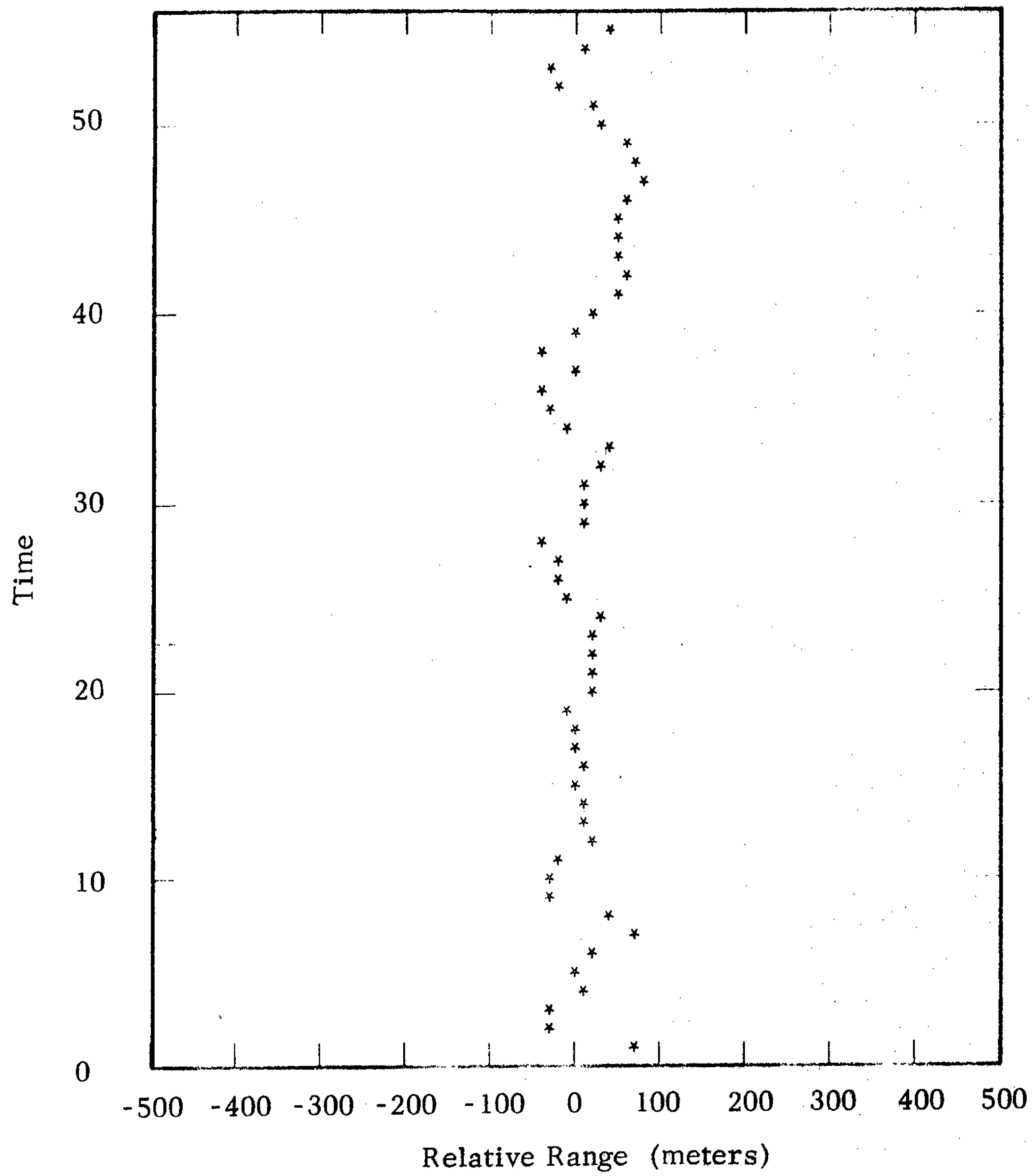

Clutter = 0%	α_1 = 0.80	σ_N = 20
Missed Returns = 0%	α_2 = -0.20	$2\sigma_X$ = 55

Fig. C-3. Unsteady target track.

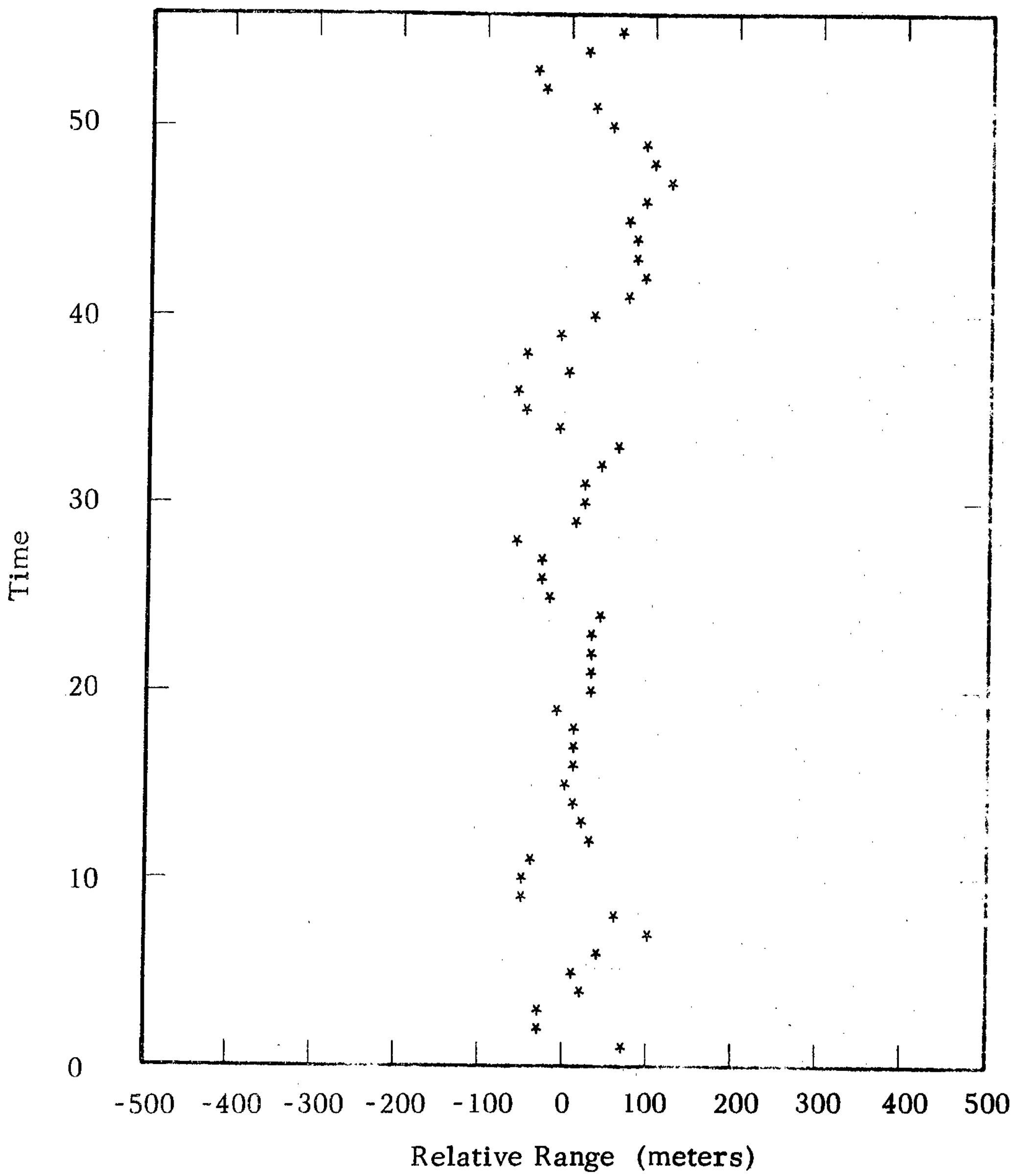

Clutter = 0% α_1 = 0.80 σ_N = 30

Missed Returns = 0% α_2 = -0.20 $2\sigma_X$ = 82

Fig. C-4. Unsteady target track.

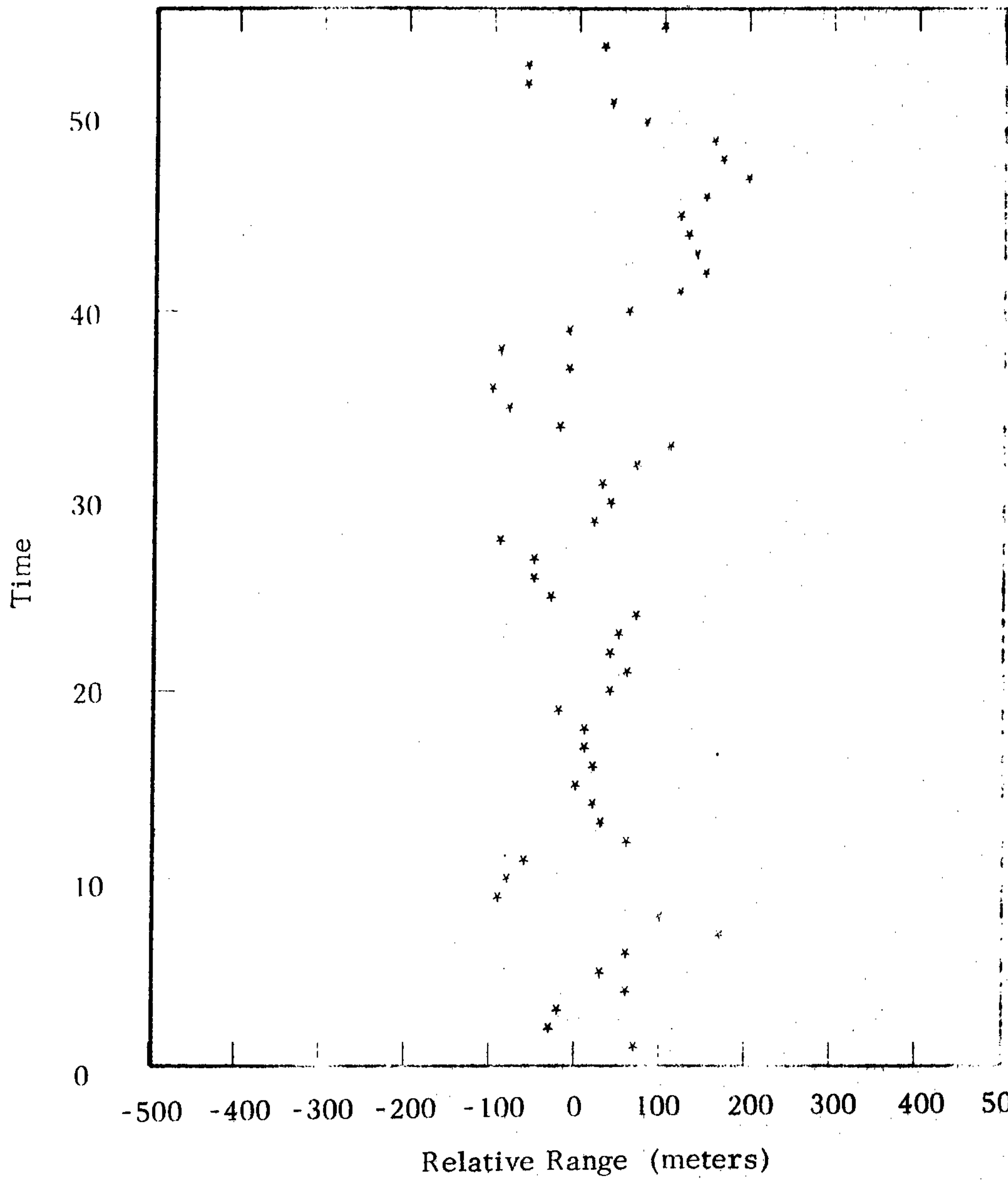

Clutter = 0% α_1 = 0.80 σ_N = 50

Missed Returns = 0% α_2 = -0.20 $2\sigma_X$ = 137

Fig. C-5. Unsteady target track.

PA-385 (C-6)

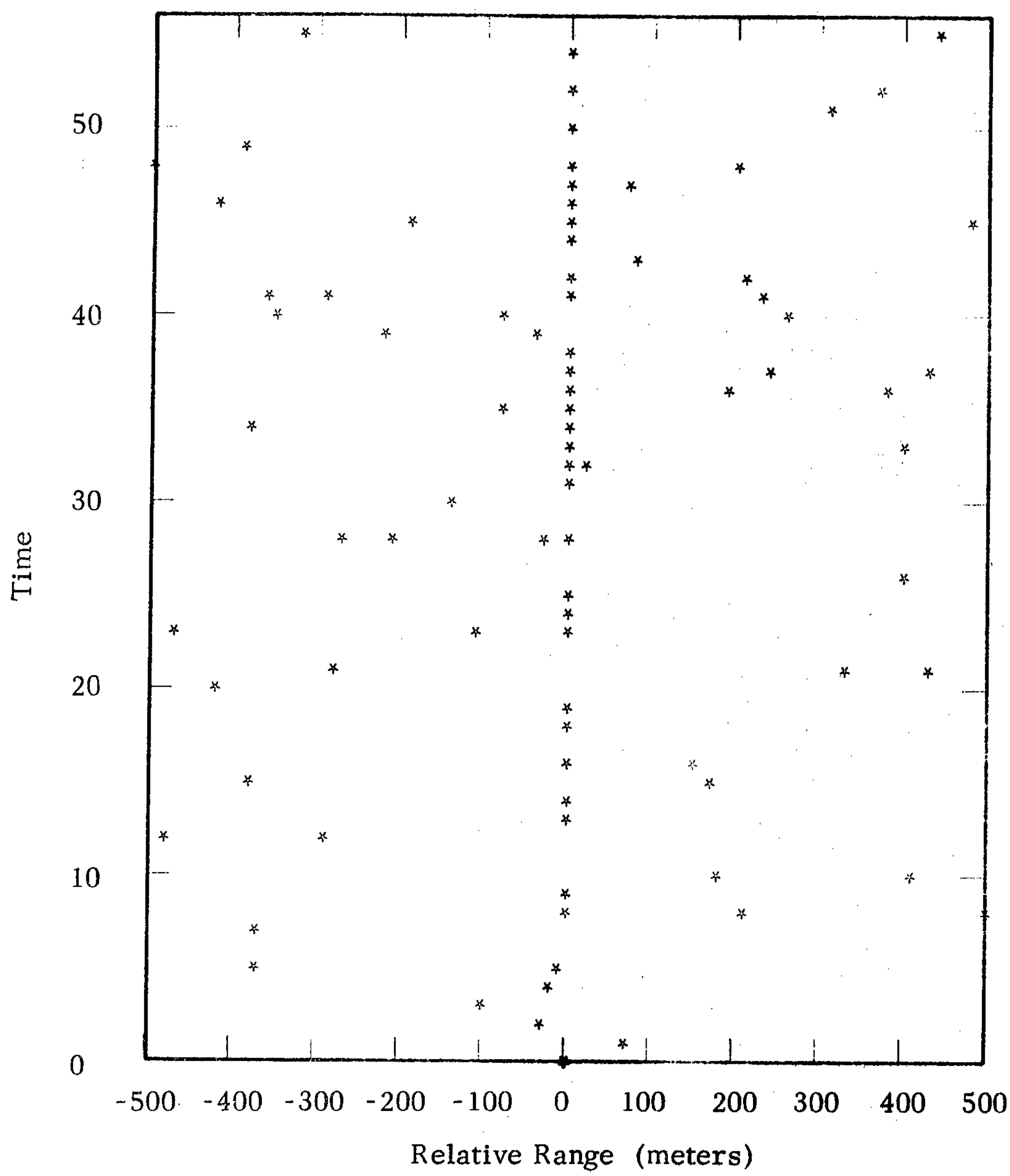

Clutter = 1% α_1 = 0.80 σ_N = 0

Missed Returns = 50% α_2 = -0.20 $2\sigma_X$ = 0

Fig. C-6. Degraded RTI.

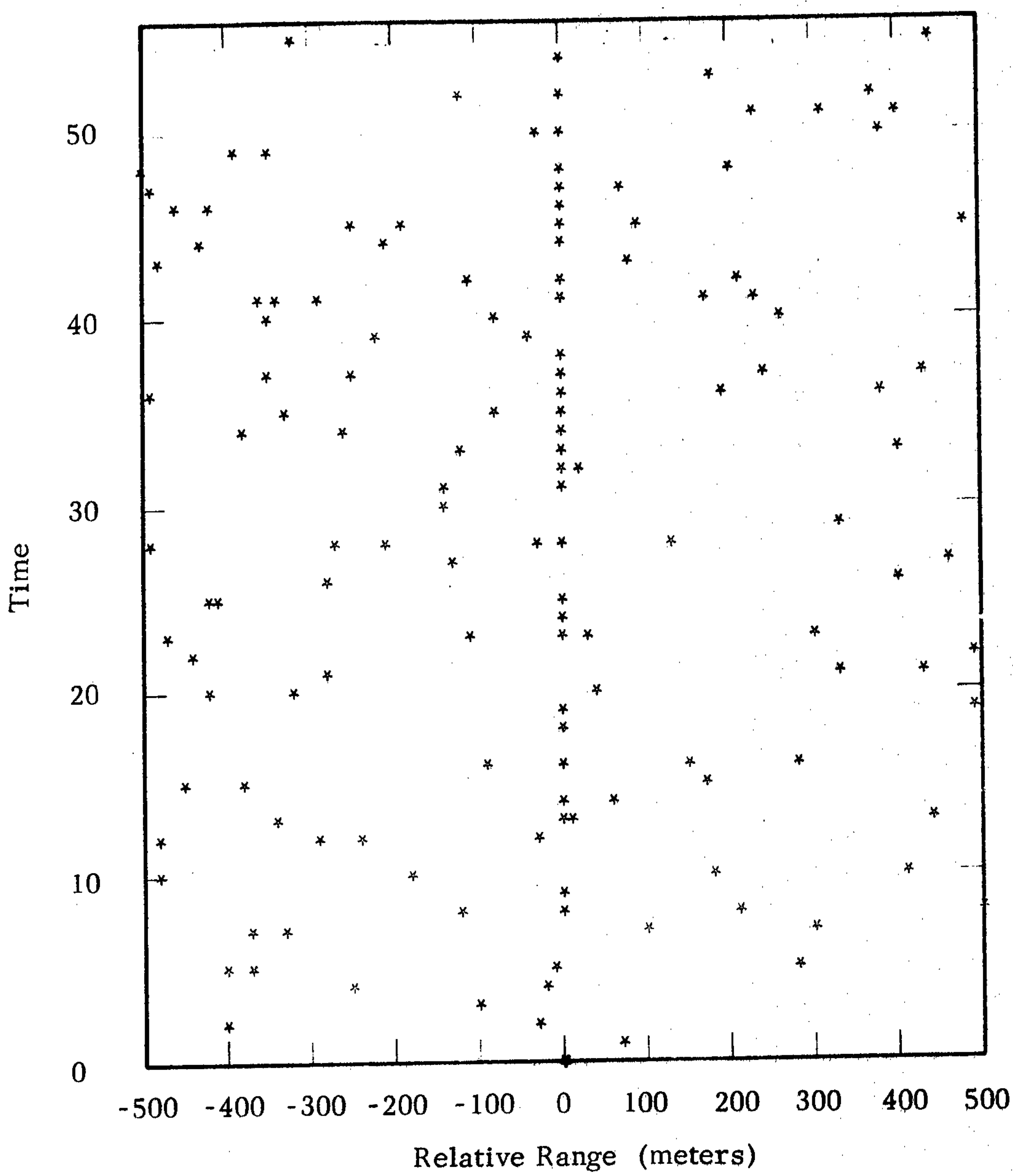

Clutter = 2% α_1 = 0.80 σ_N = 0

Missed Returns = 50% α_2 = -0.20 $2\sigma_X$ = 0

Fig. C-7. Degraded RTI.

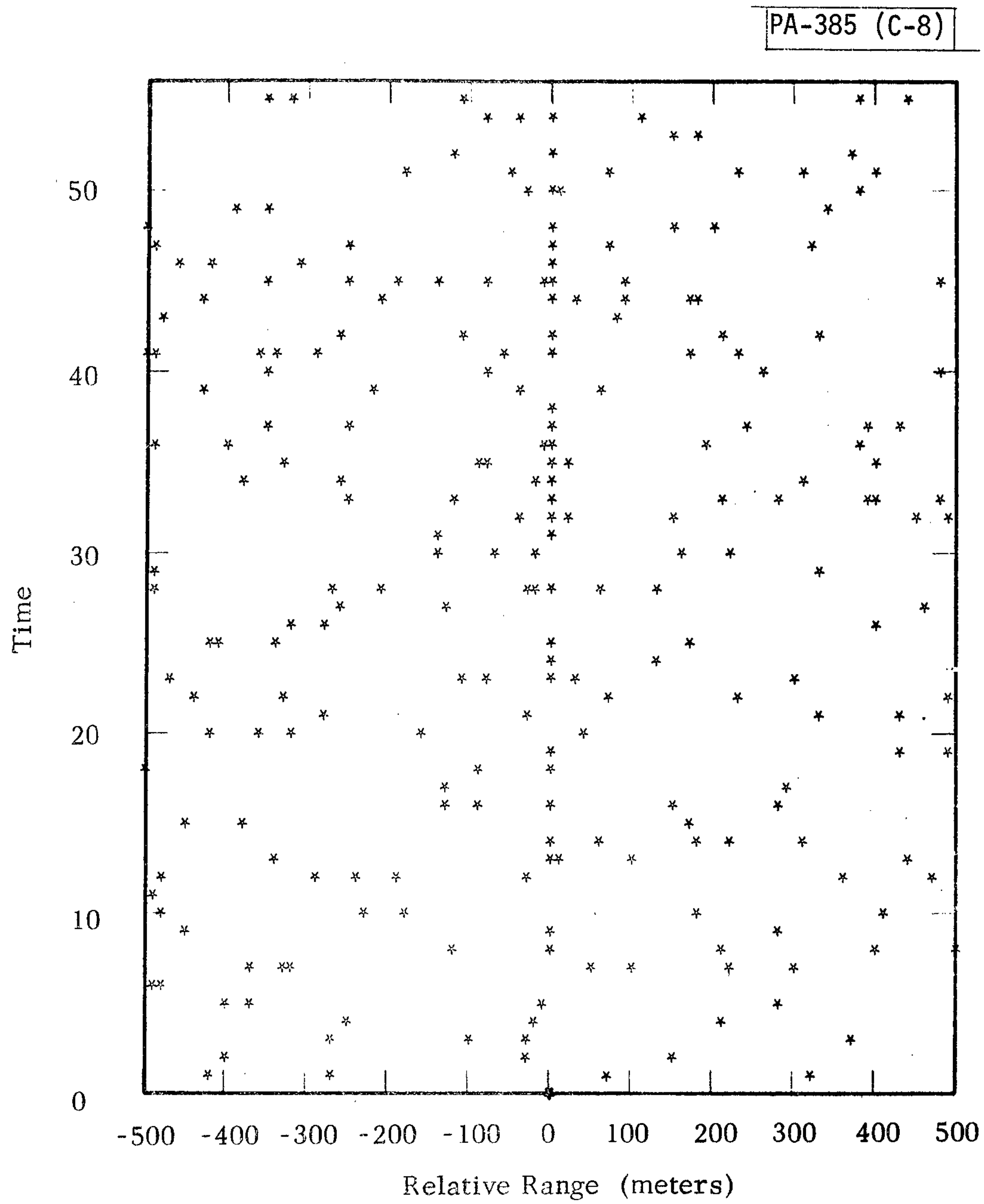

Clutter = 4% α_1 = 0.80 σ_N = 0

Missed Returns = 50% α_2 = -0.20 $2\sigma_X$ = 0

Fig. C-8. Degraded RTI.

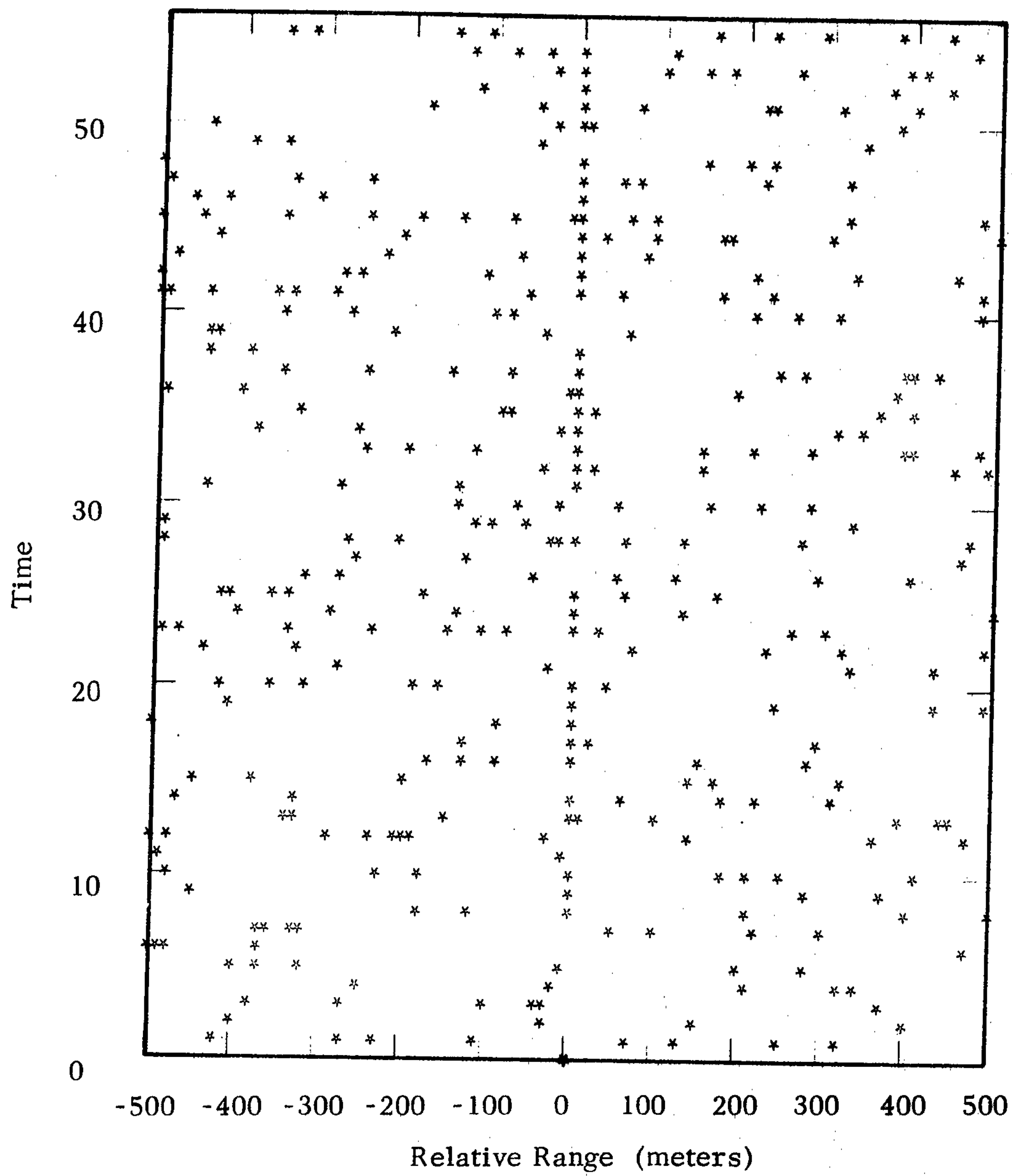

Clutter = 6% α_1 = 0.80 σ_N = 0

Missed Returns = 40% α_2 = -0.20 $2\sigma_X$ = 0

Fig. C-9. Degraded RTI.

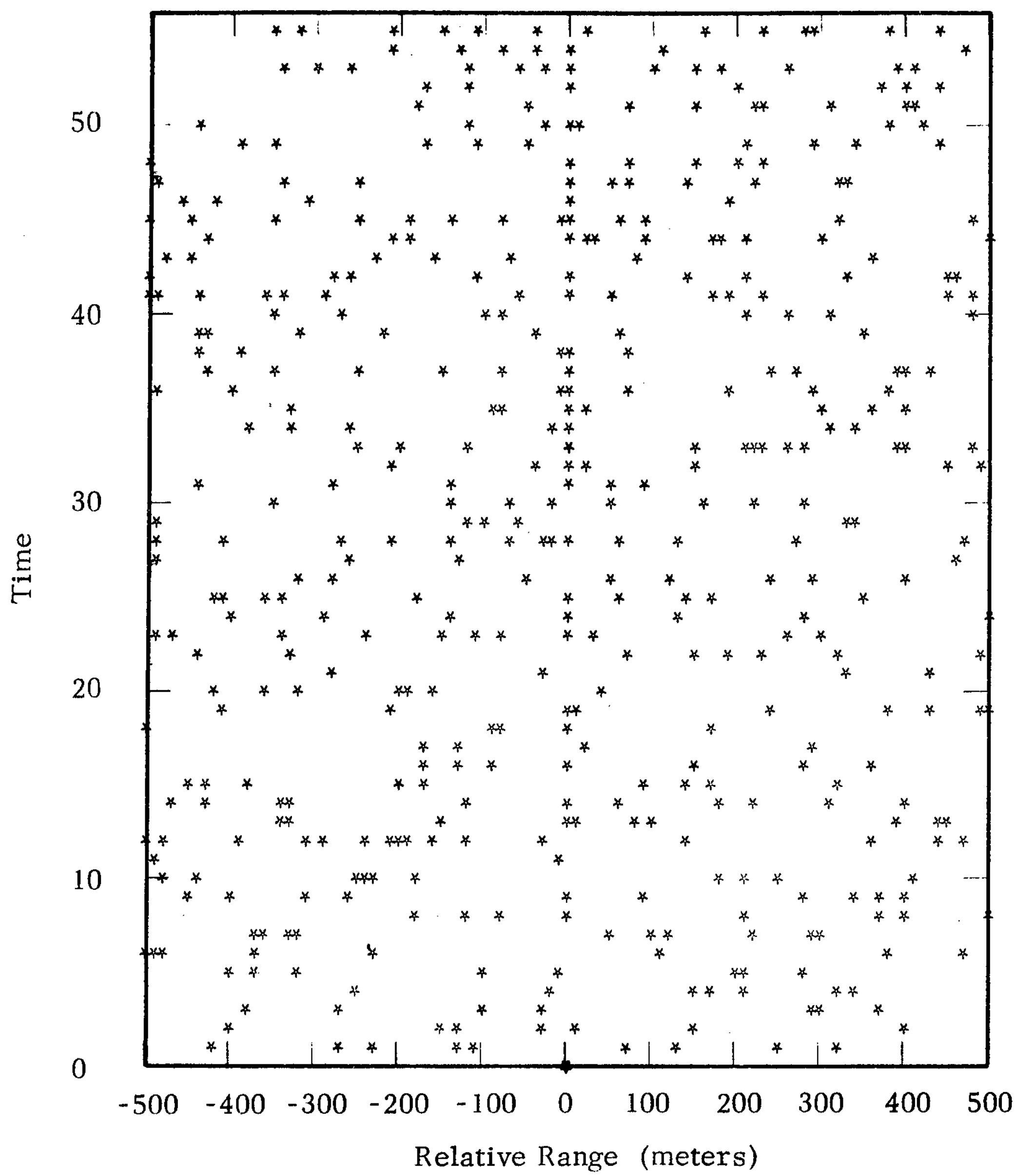

Clutter = 8% α_1 = 0.80 σ_N = 0

Missed Returns = 50% α_2 = -0.20 $2\sigma_X$ = 0

Fig. C-10. Degraded RTI.

PA-385 (C-11)

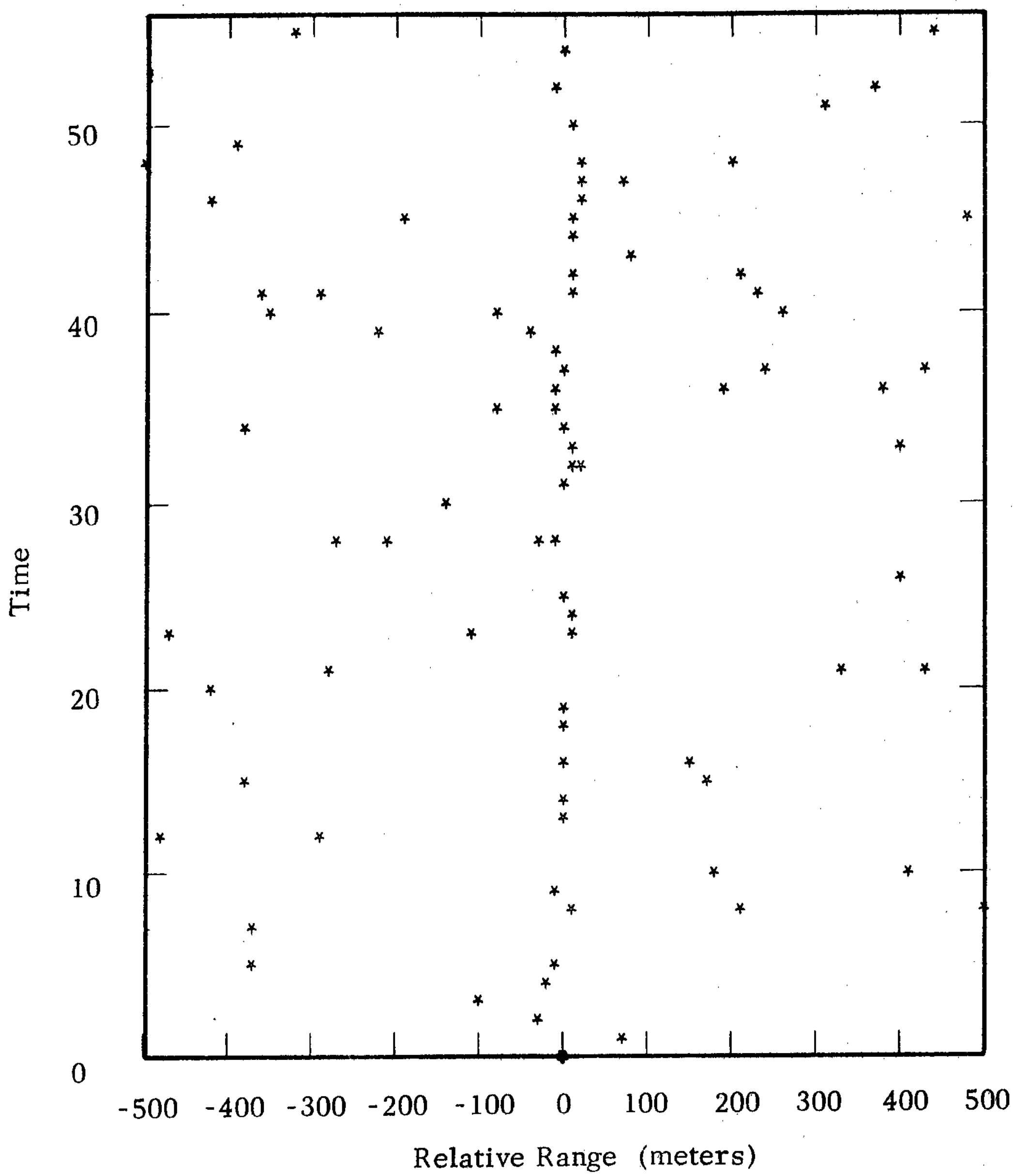

Clutter = 1% α_1 = 0.80 σ_N = 5

Missed Returns = 50% α_2 = -0.20 $2\sigma_X$ = 14

Fig. C-11. Degraded RTI.

PA-385 (C-12)

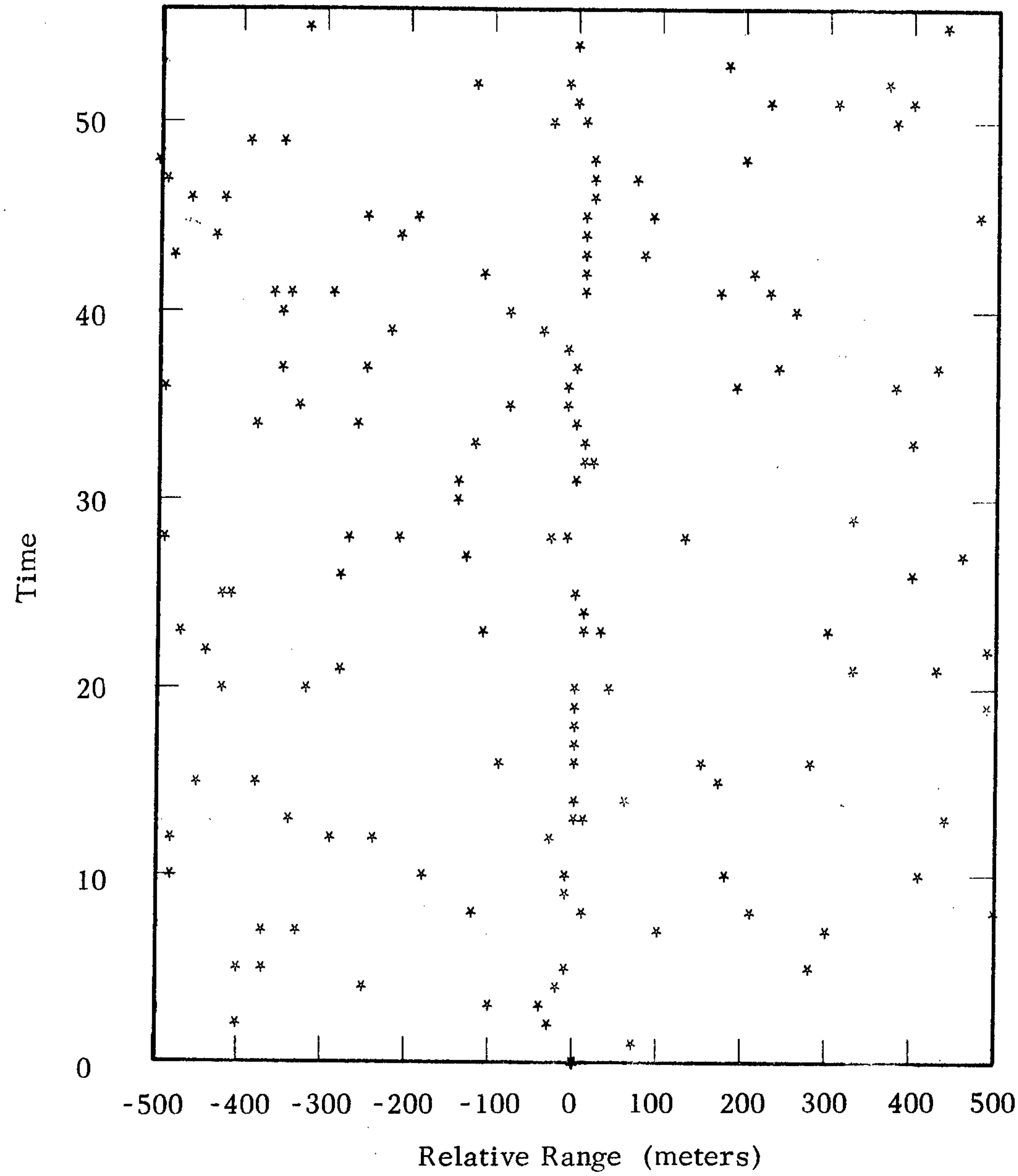

Clutter = 2% α_1 = 0.80 σ_N = 5

Missed Returns = 40% α_2 = -0.20 $2\sigma_X$ = 14

Fig. C-12. Degraded RTI.

PA-385 (C-13)

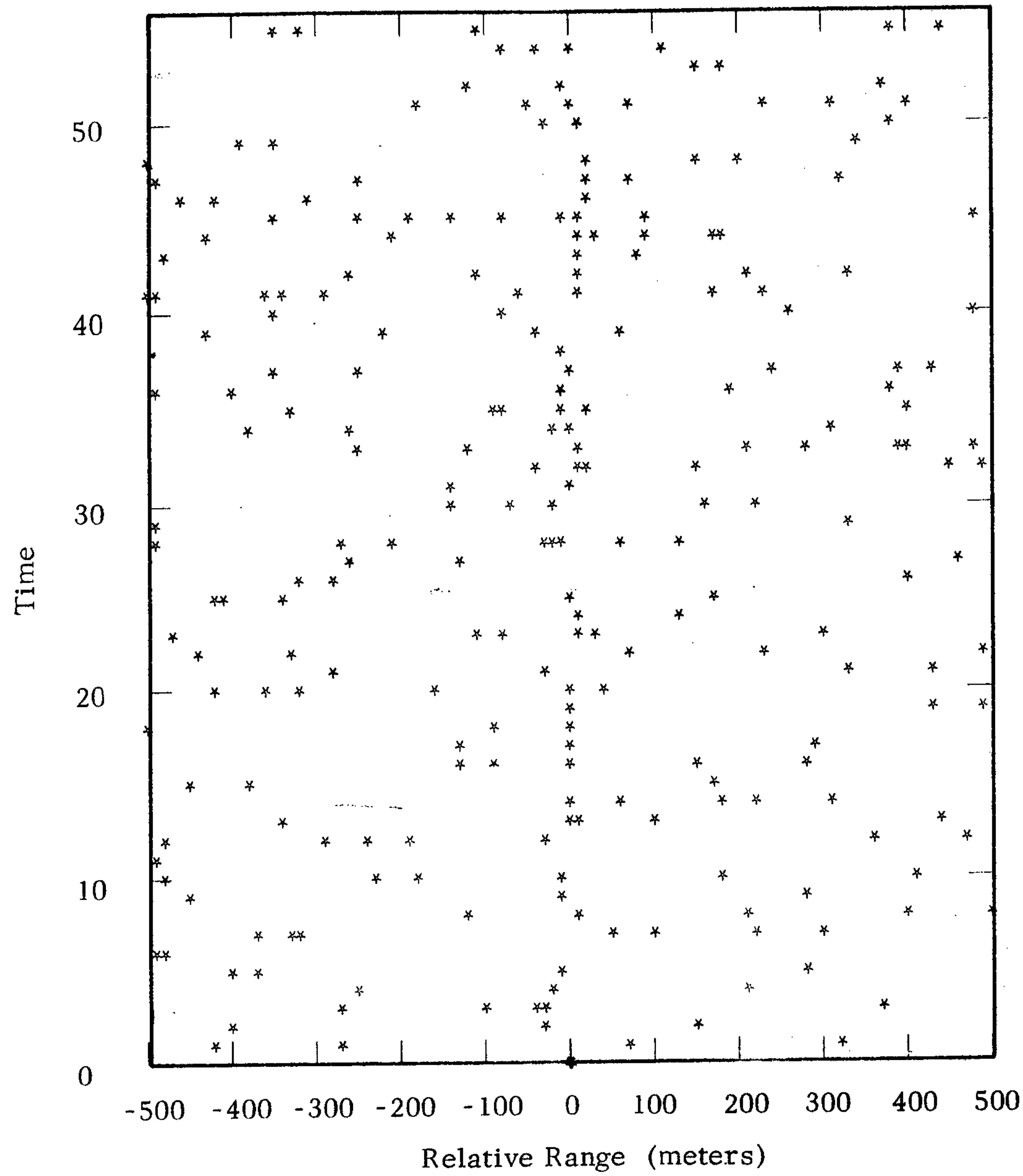

Clutter = 4% α_1 = 0.80 σ_N = 5

Missed Returns = 40% α_2 = -0.20 $2\sigma_X$ = 14

Fig. C-13. Degraded RTI.

PA-385 (C-14)

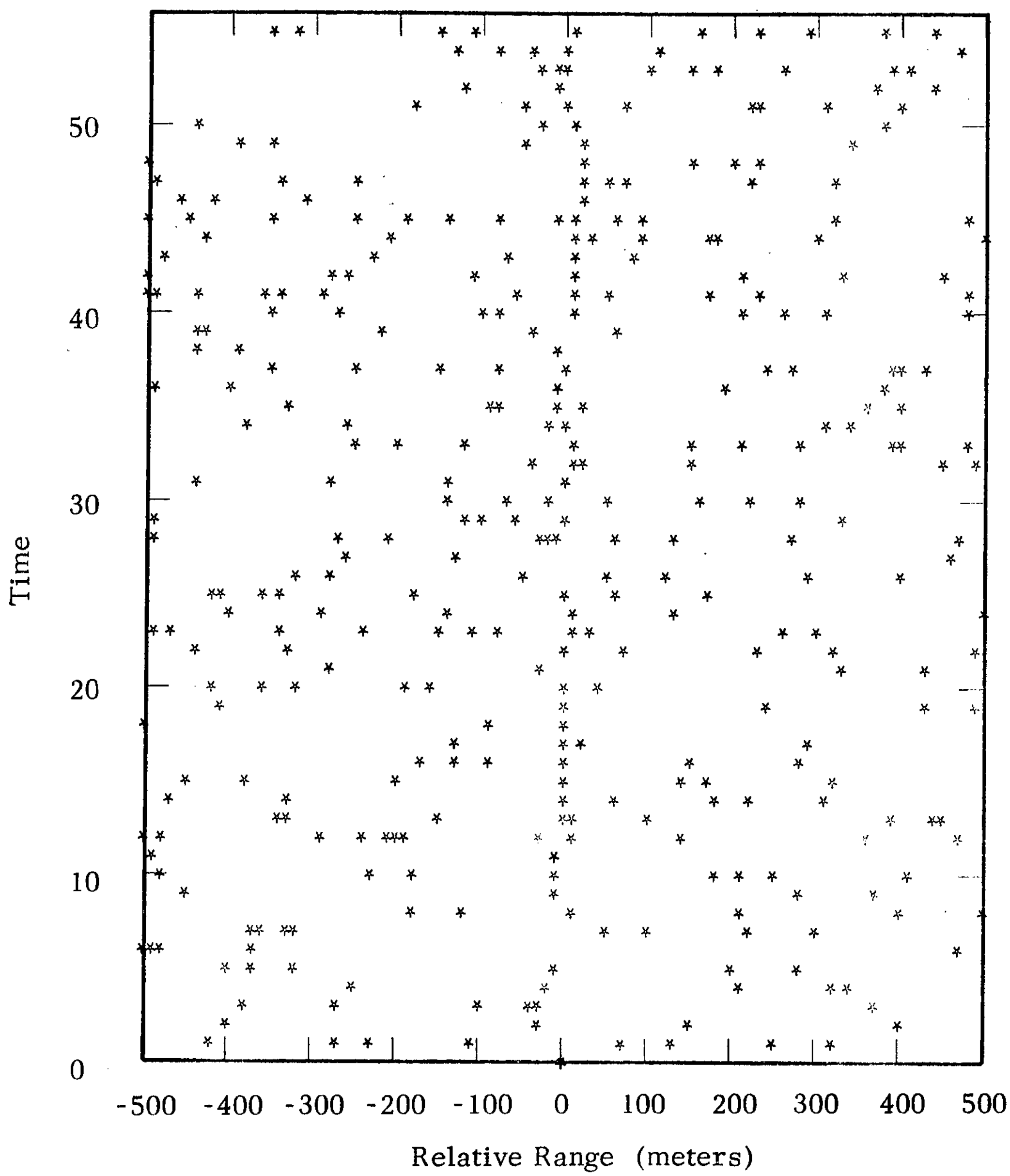

Clutter = 6% α_1 = 0.80 σ_N = 5

Missed Returns = 10% α_2 = -0.20 $2\sigma_X$ = 14

Fig. C-14. Degraded RTI.

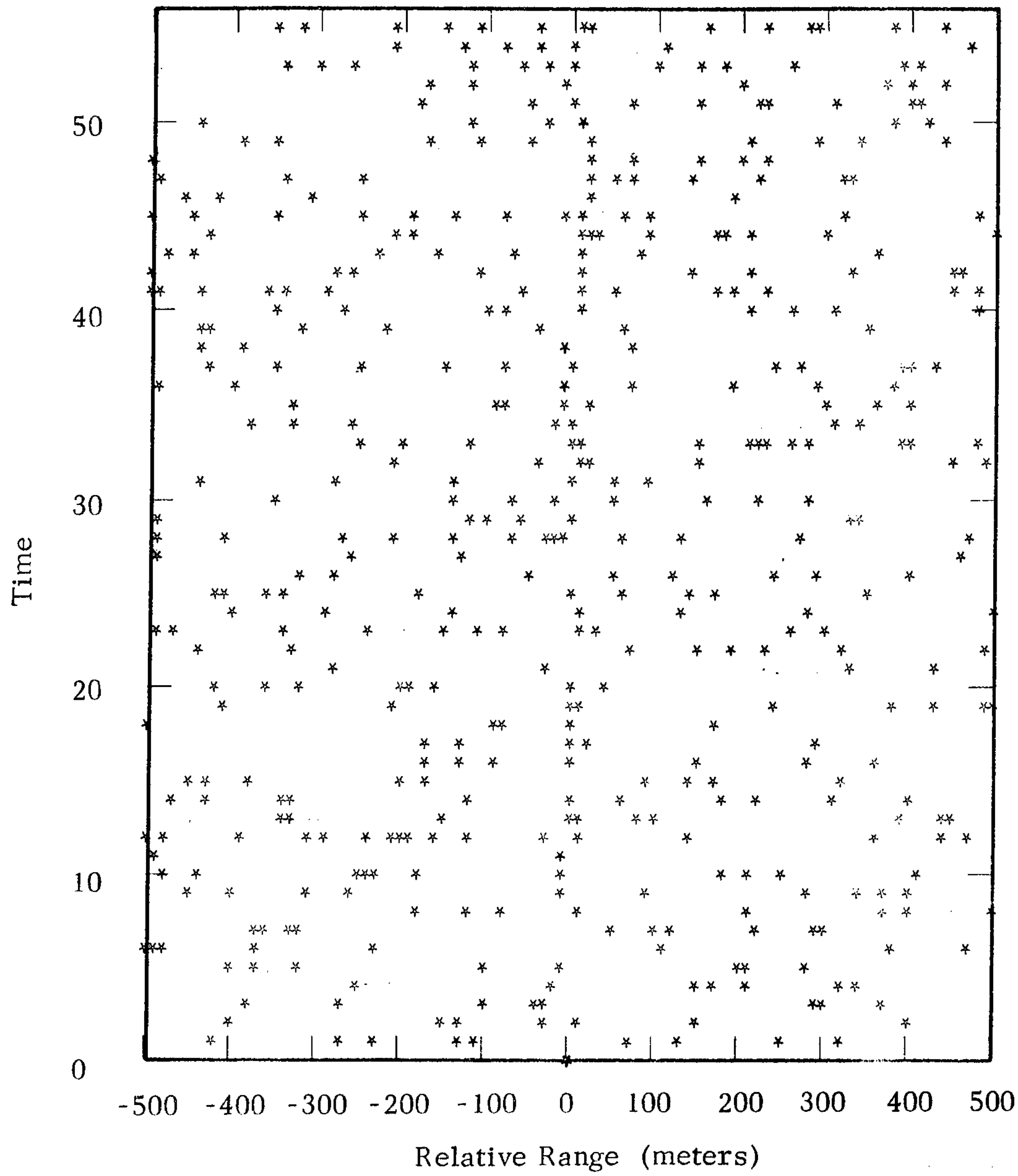

Clutter = 8% α_1 = 0.80 σ_N = 5

Missed Returns = 20% α_2 = -0.20 $2\sigma_X$ = 14

Fig. C-15. Degraded RTI.

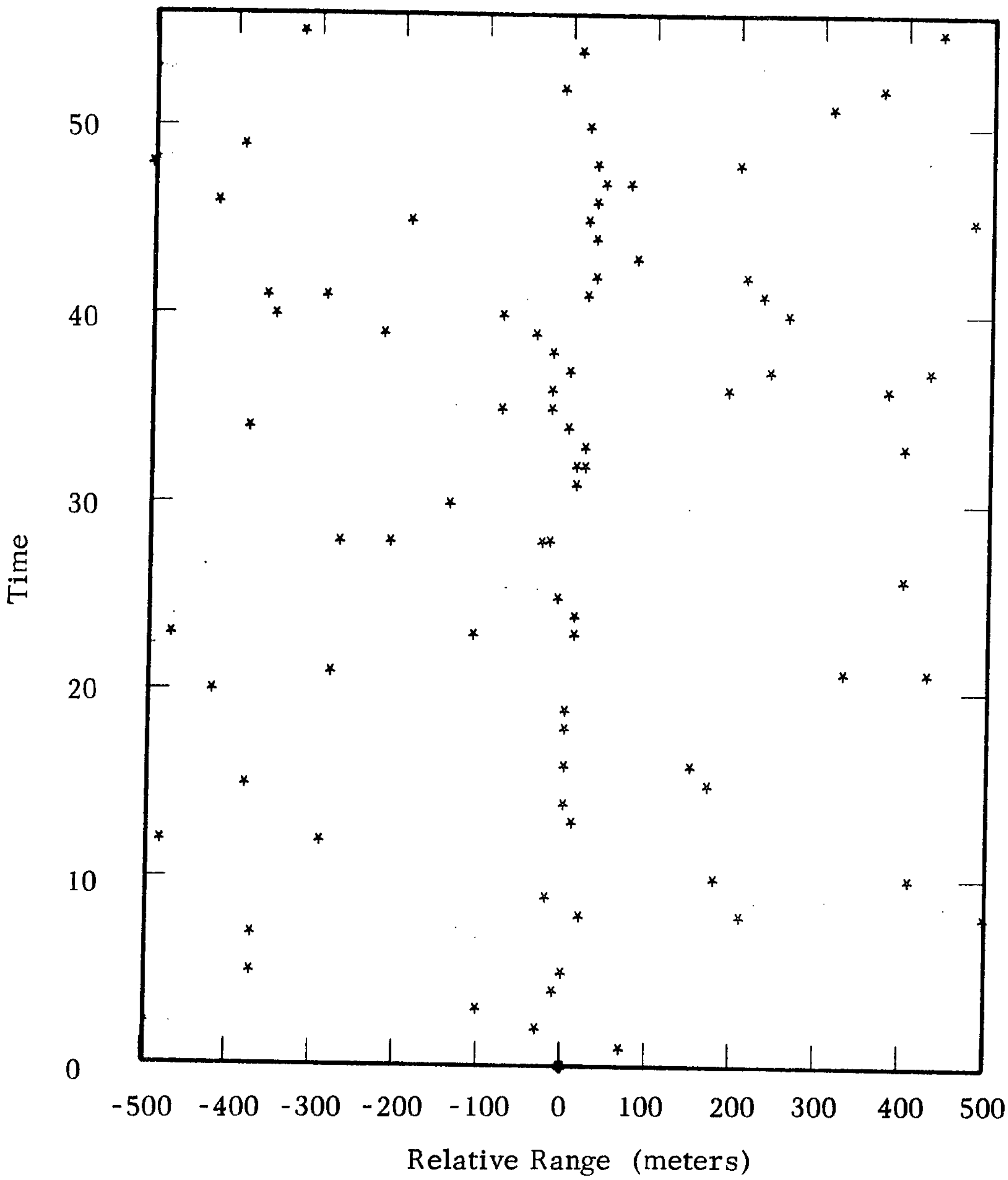

Clutter = 1% α_1 = 0.80 σ_N = 10

Missed Returns = 50% α_2 = -0.20 $2\sigma_X$ = 27

Fig. C-16. Degraded RTI.

PA-385(C-17)

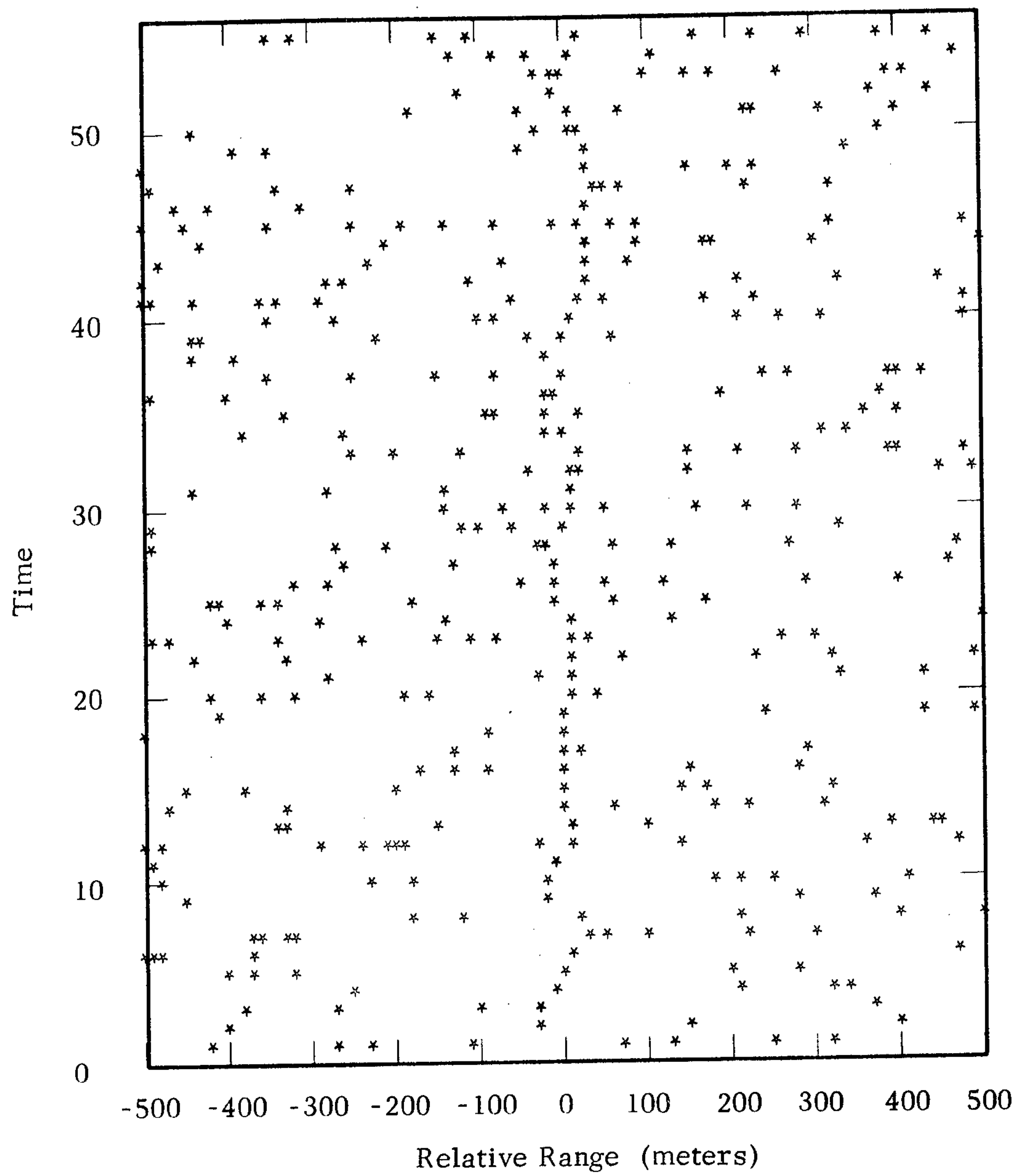

Clutter = 6% α_1 = 0.80 σ_N = 10

Missed Returns = 0% α_2 = -0.20 $2\sigma_X$ = 27

Fig. C-17. Degraded RTI.

PA-385(C-18)

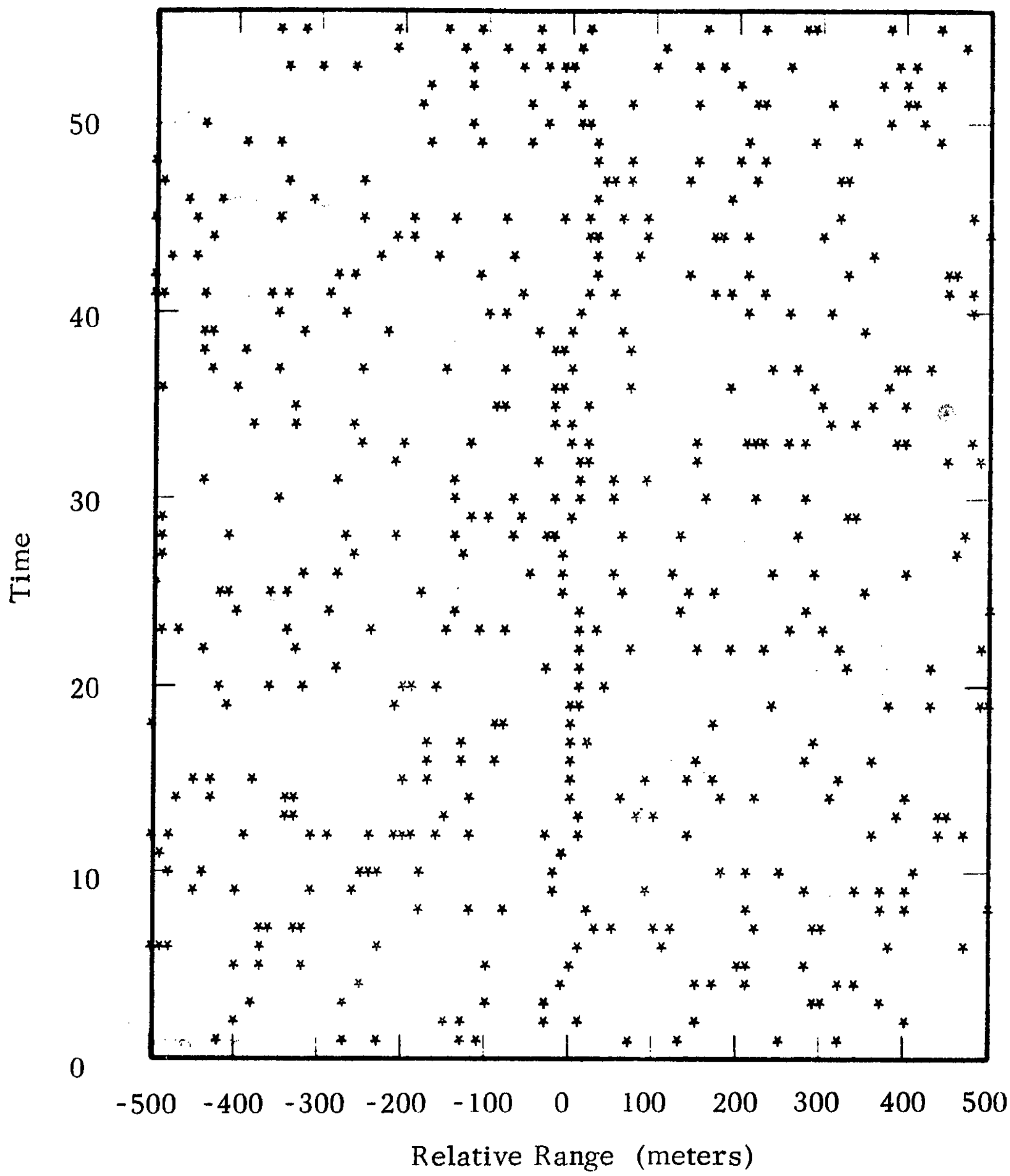

Clutter = 8% α_1 = 0.80 σ_N = 10

Missed Returns = 0% α_2 = -0.20 $2\sigma_X$ = 27

Fig. C-18. Degraded RTI.

PA-385(C-19)

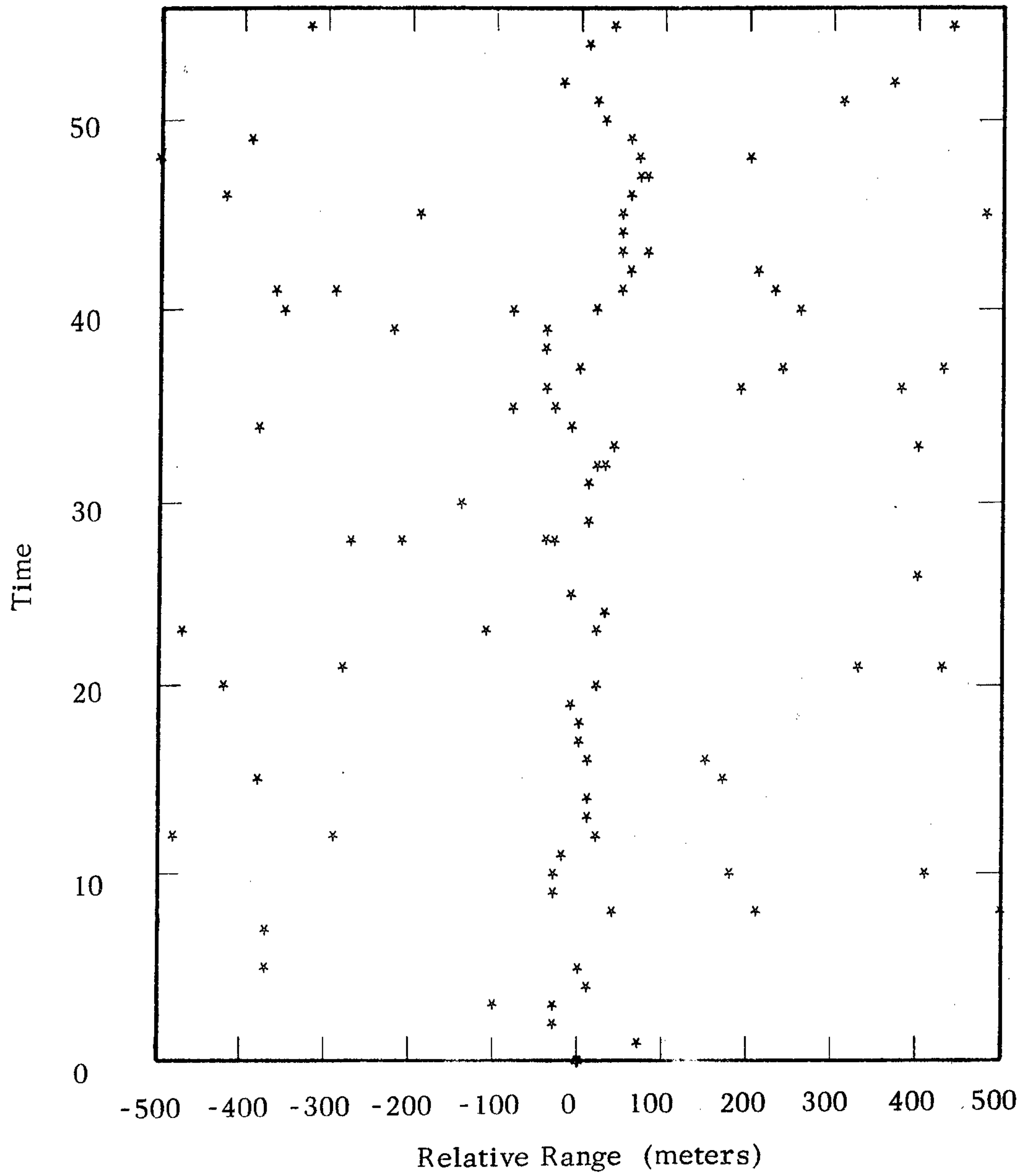

Clutter = 1% α_1 = 0.80 σ_N = 20

Missed Returns = 20% α_2 = -0.20 $2\sigma_X$ = 55

Fig. C-19. Degraded RTI.

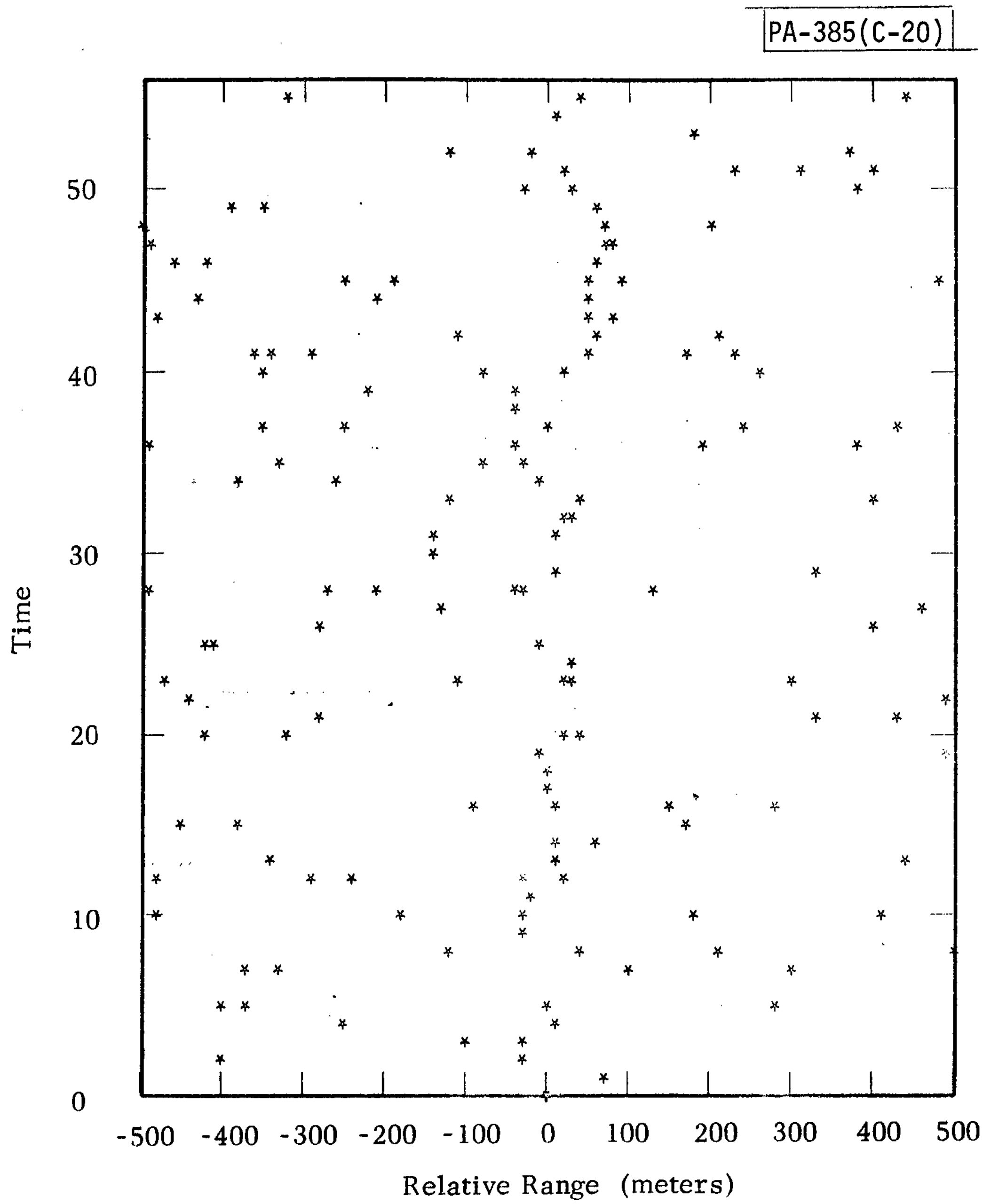

Clutter = 2% α_1 = 0.80 σ_N = 20

Missed Returns = 20% α_2 = -0.20 $2\sigma_X$ = 55

Fig. C-20. Degraded RTI.

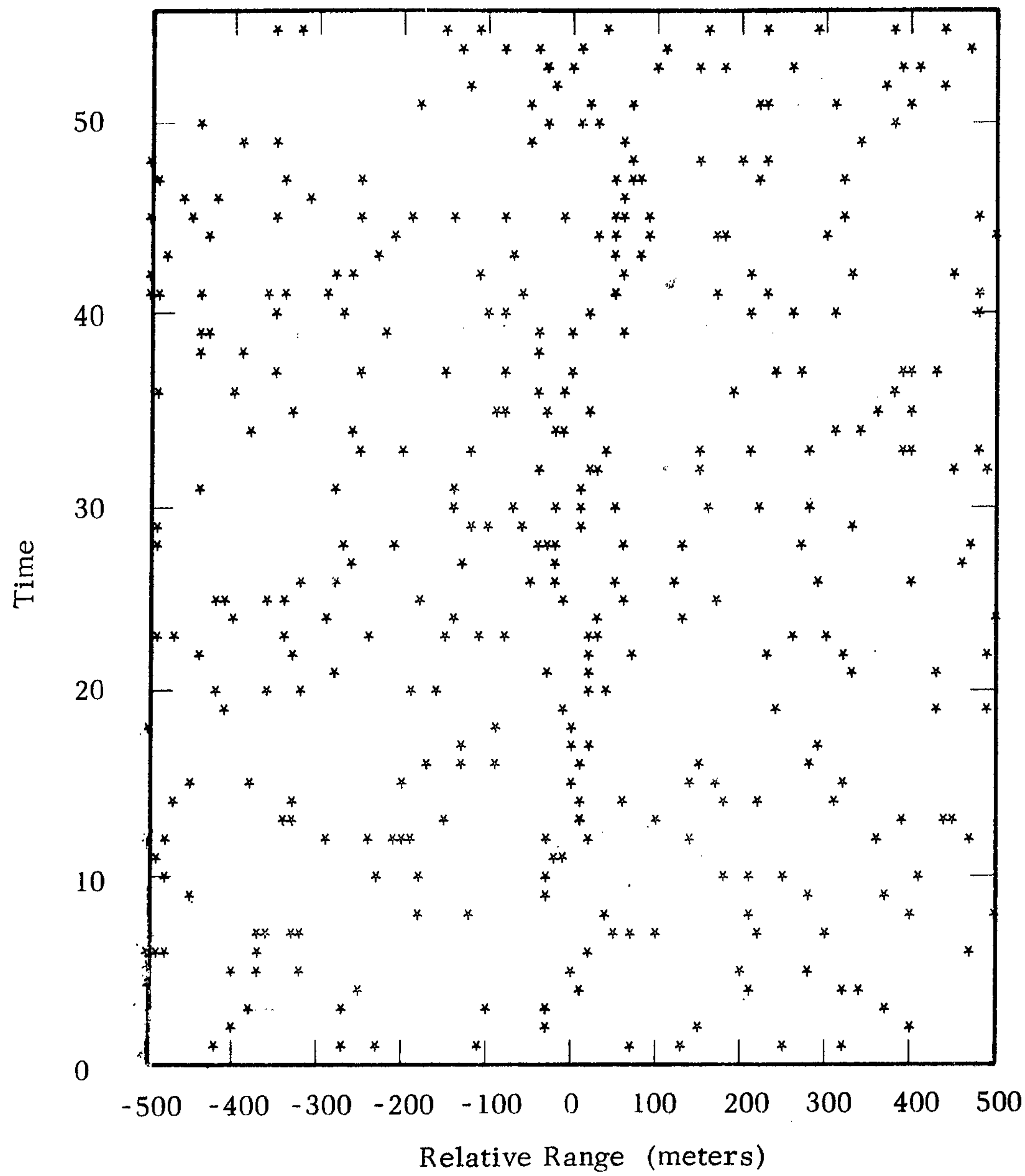

Clutter = 6% α_1 = 0.80 σ_N = 20

Missed Returns = 0% α_2 = -0.20 $2\sigma_X$ = 55

Fig. C-21. Degraded RTI.

PA-385(C-22)

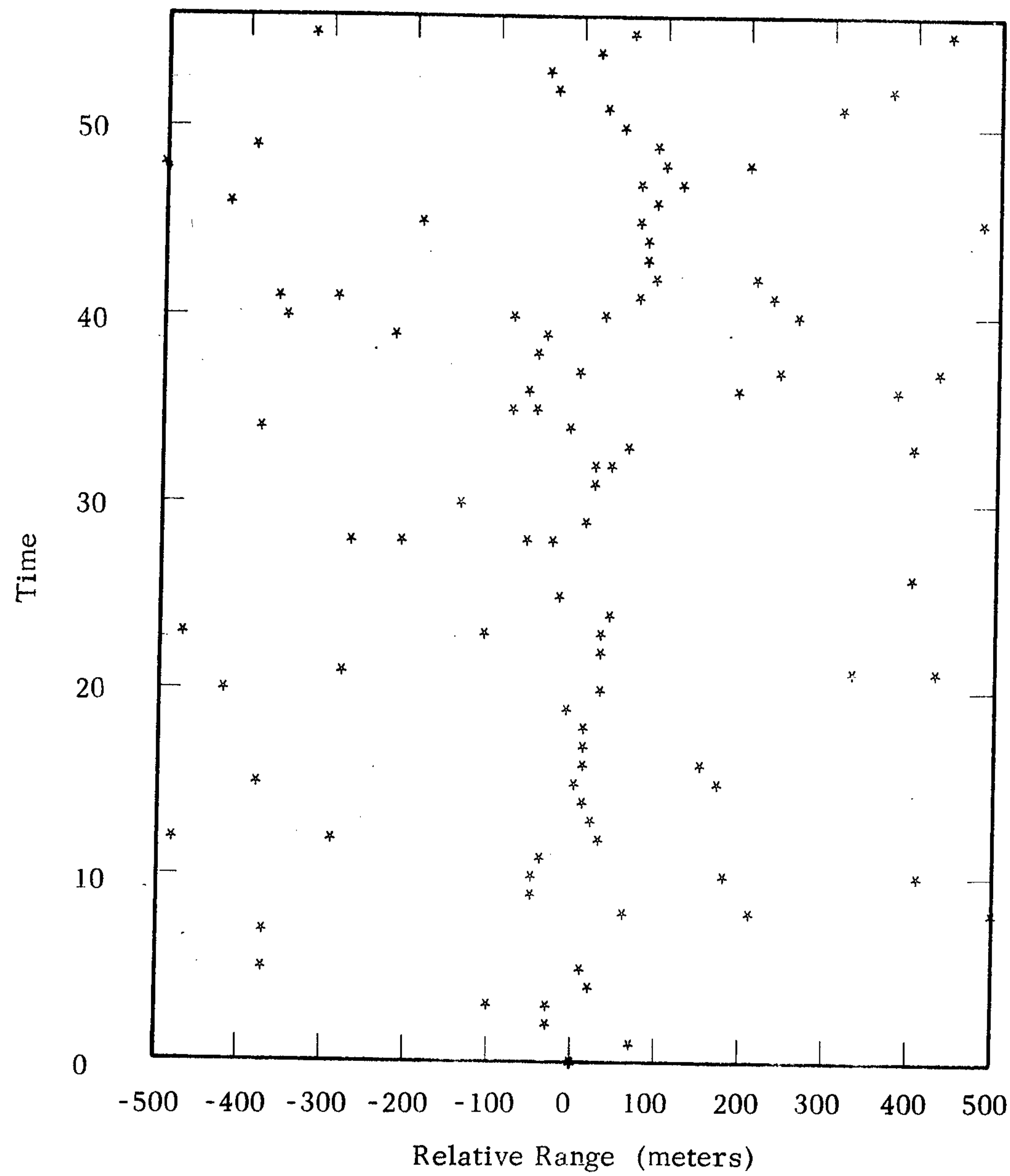

Clutter = 1%	α_1 = 0.80	σ_N = 30
Missed Returns = 10%	α_2 = -0.20	$2\sigma_X$ = 82

Fig. C-22. Degraded RTI.

PA-385(C-23)

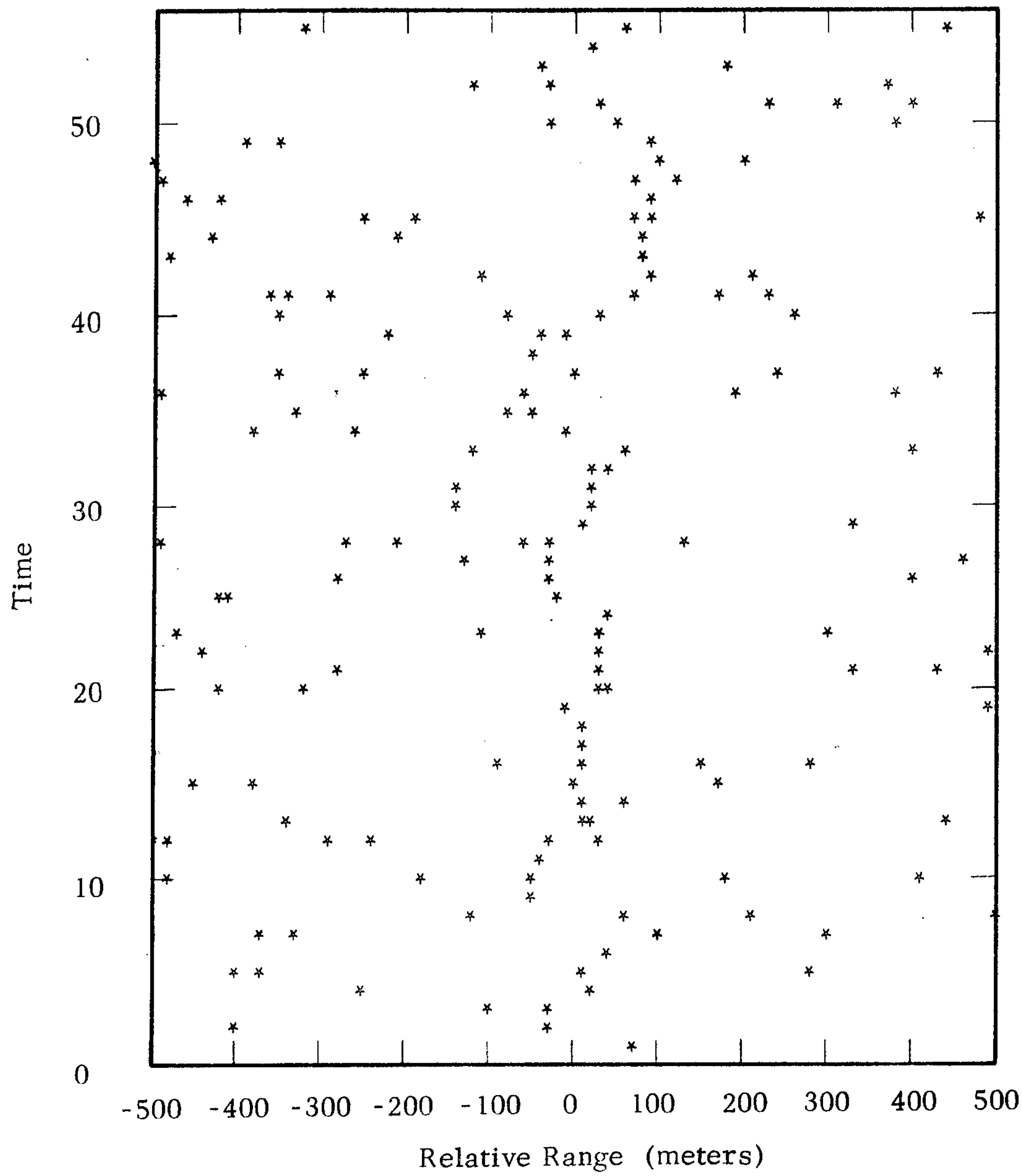

Clutter = 2% $\quad \alpha_1 = 0.80 \quad \sigma_N = 30$

Missed Returns = 0% $\quad \alpha_2 = -0.20 \quad 2\sigma_X = 82$

Fig. C-23. Degraded RTI.

PA-385(C-24)

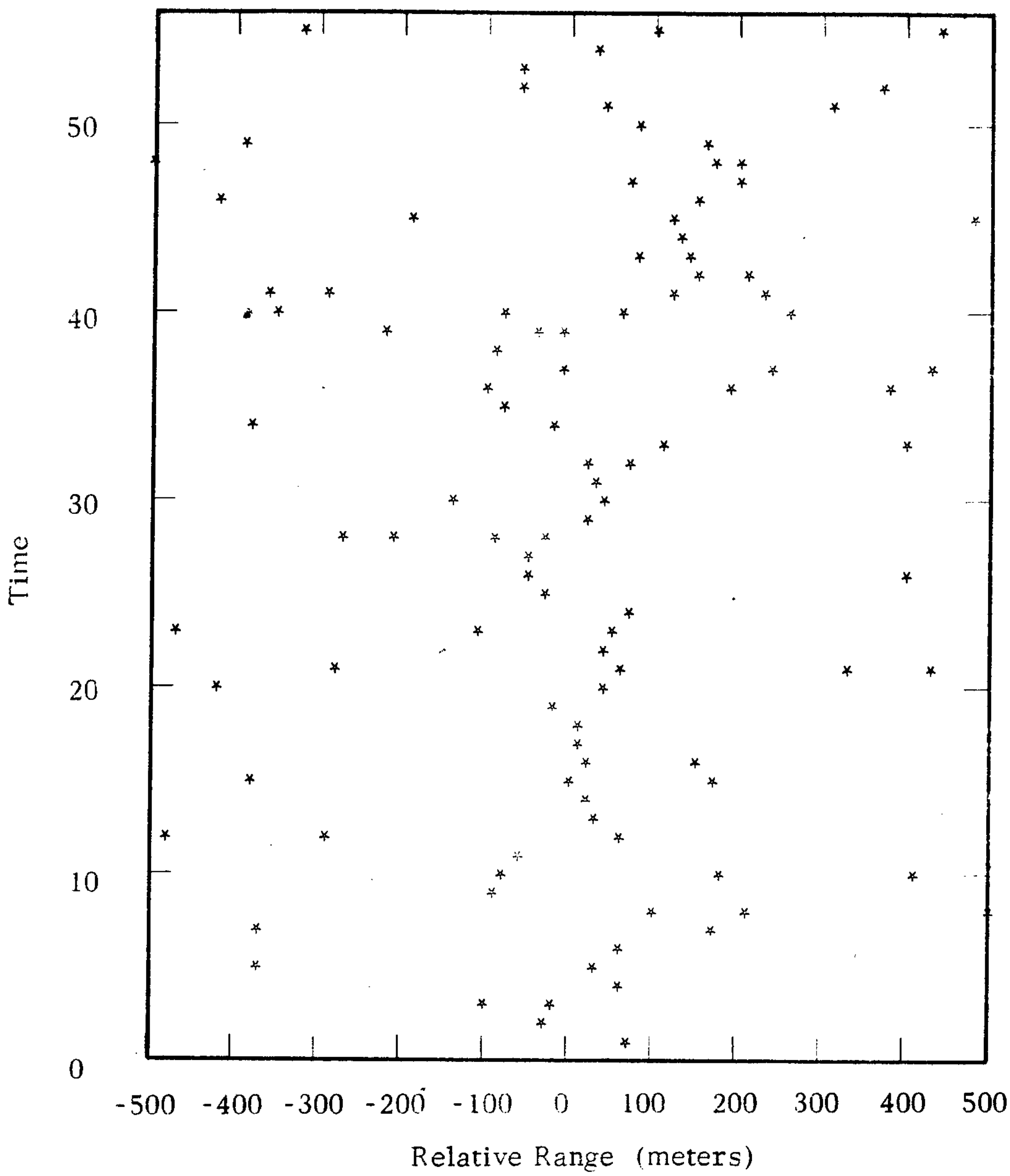

Clutter = 1% α_1 = 0.80 σ_N = 50

Missed Returns = 0% α_2 = -0.20 $2\sigma_X$ = 137

Fig. C-24. Degraded RTI.